

UNIVERSIDADE DE BRASÍLIA
FACULDADE DE TECNOLOGIA
DEPARTAMENTO DE ENGENHARIA ELÉTRICA

ECONOMIC DISPATCH PROBLEM SOLUTION VIA
HOLOMORPHIC EMBEDDING METHOD

ANA CATARINA SALLES RAMOS

ORIENTADOR: FRANCISCO DAMASCENO FREITAS

DISSERTAÇÃO DE MESTRADO EM
ENGENHARIA ELÉTRICA

BRASÍLIA/DF: 03 DE OUTUBRO - 2019

UNIVERSIDADE DE BRASÍLIA
FACULDADE DE TECNOLOGIA
DEPARTAMENTO DE ENGENHARIA ELÉTRICA

ECONOMIC DISPATCH PROBLEM SOLUTION VIA HOLOMORPHIC
EMBEDDING METHOD

ANA CATARINA SALLES RAMOS

DISSERTAÇÃO DE MESTRADO SUBMETIDA AO DEPARTAMENTO DE ENGENHARIA
ELÉTRICA DA FACULDADE DE TECNOLOGIA DA UNIVERSIDADE DE BRASÍLIA, COMO
PARTE DOS REQUISITOS NECESSÁRIOS PARA A OBTENÇÃO DO GRAU DE MESTRE.

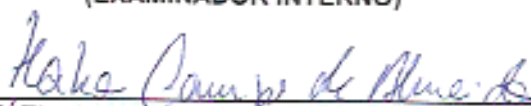
APROVADA POR:



FRANCISCO DAMASCENO FREITAS
(ORIENTADOR)



FELIPE VIGOLVINO LOPES
(EXAMINADOR INTERNO)



KÁTIA CAMPOS DE ALMEIDA, Dra., UFSC
(EXAMINADOR EXTERNO)

Brasília, 03 de outubro de 2019.

FICHA CATALOGRÁFICA

SALLES RAMOS, ANA CATARINA

ECONOMIC DISPATCH PROBLEM

SOLUTION VIA HOLOMORPHIC

EMBEDDING METHOD

[Distrito Federal] 2019.

xiii, 89 páginas, 297 mm (ENE/FT/UnB, Mestre, Engenharia Elétrica,
2019). Dissertação de Mestrado - Universidade de Brasília.

Faculdade de Tecnologia. Departamento de Engenharia Elétrica.

1. Despacho Econômico

2. Métodos Numéricos

3. Métodos Não-Iterativos

4. Método Holomorphic Embedding

I. ENE/FT/UnB

II. Título

REFERÊNCIA BIBLIOGRÁFICA

Salles Ramos, A. C. (2019). ECONOMIC DISPATCH PROBLEM SOLUTION VIA HOLOMORPHIC EMBEDDING METHOD. Dissertação de Mestrado, Publicação 726/19 ENE/2019, Departamento de Engenharia Elétrica, Faculdade de Tecnologia, Universidade de Brasília, Brasília, DF, 89 páginas.

CESSÃO DE DIREITOS

AUTOR: Ana Catarina Salles Ramos

TÍTULO: ECONOMIC DISPATCH PROBLEM SOLUTION VIA HOLOMORPHIC EMBEDDING METHOD

GRAU / ANO: Mestre em Engenharia Elétrica / 2019

É concedida à Universidade de Brasília permissão para reproduzir cópias desta dissertação de mestrado e para emprestar tais cópias somente para propósitos acadêmicos e científicos. O autor reserva outros direitos de publicação e nenhuma parte desta dissertação de mestrado pode ser reproduzida sem a autorização por escrito do autor.

Ana Catarina Salles Ramos

Brasília – DF

AGRADECIMENTOS

Agradeço aos meus pais por todo o apoio dado ao longo do meu mestrado.

Agradeço aos meus irmãos pelas distrações e confidências tão bem vindas.

Agradeço aos meus amigos sempre presentes e dispostos a ajudar.

Agradeço aos professores que contribuíram para minha formação de mestre, durante o mestrado em Engenharia Elétrica. Agradeço, em especial, ao Professor Francisco Damasceno pelo seu o apoio e suas orientações.

Agradeço à UnB e o Departamento de Engenharia Elétrica pela oportunidade de desenvolver este trabalho.

Agradeço aos colegas e professores no LabRei pela acolhida.

Agradeço ao Prof. Dr. Felipe e à Profa. Dra. Kátia por aceitarem a participar da minha banca.

Ana C. S. Ramos

RESUMO

Este trabalho propõe uma técnica de solução alternativa para o Problema do Despacho Econômico (PDE) de máquinas térmicas em sistemas elétricos de potência com perdas de transmissão. A técnica empregada é chamada de *Holomorphic Embedding* (Adaptação Holomórfica). Uma vez levantadas as equações do PDE, o problema é adaptado de forma holomórfica. Este processo é feito mediante o cálculo de um termo obtido a partir do resíduo inicial do sistema de equações não-lineares e de inclusão de um fator de escala. O fator de escala é tal que quando ajustado para o valor unitário, permite a obtenção da solução do sistema. O resíduo inicial é calculado a partir de uma estimativa para obtenção da solução do PDE. Na abordagem holomórfica, esta estimativa inicial é denominada "solução semente". Sua estimativa, por sua vez, foi realizada determinando-se a solução do PDE formulado sem as perdas de transmissão. O método utilizado emprega uma formulação que preconiza a obtenção de uma série de Taylor com número reduzido de coeficientes. A série é então tratada e aproximada por uma fração racional, denominada aproximação de Padé. Este é um fator positivo, pois polinômios com elevado grau tendem a apresentar coeficientes com valores absolutos muitíssimo reduzidos (elevados). Neste caso, a busca por uma solução dos sistemas de equações não-lineares pode estagnar em um valor distante da solução de interesse. Por isso, caso a solução com polinômio de baixa ordem se apresente com precisão insuficiente, é feito um processo de reinicialização dos cálculos dos coeficientes. Porém, agora, usando como solução semente computada a partir da aproximação de Padé mais atualizada, considerando-se o fator de escala em seu valor unitário. O processo de otimização dos custos para geração de potência leva em conta os limites operacionais destas variáveis. Resolve-se o mesmo PDE pelo método clássico de Newton-Raphson. A finalidade é ter uma referência computacional para se avaliar o desempenho da técnica proposta. Simulações computacionais em três sistemas testes, considerando algumas topologias diferentes para cada um deles, servem como meios para se avaliar o desempenho da solução do PDE mediante a técnica de adaptação holomórfica. Os resultados obtidos demonstram que o método proposto apresenta resultados similares aos encontrados pela solução com o tradicional método de Newton-Raphson. A vantagem da técnica proposta reside no fato que uma abordagem recursiva é usada para determinar os coeficientes da série de Taylor e na sua robustez para determinação da solução do problema, conforme aferido mediante monitoramento dos resíduos da solução.

Palavras-chave: Despacho econômico, adaptação holomórfica, reinicialização, método de Newton-Raphson, perdas de transmissão, série de Taylor, aproximação de Padé.

ABSTRACT

This work proposes an alternative solution technique for the Economic Dispatch Problem (EDP) for thermal generation units in lossy transmission system for electrical power systems. The Holomorphic Embedding Method (HEM) is employed to solve the nonlinear equations that arise on the EDP formulation. Once the EDP equations with transmission losses are raised, the problem is holomorphically embedded. This process is done by calculating a term obtained from the initial residual of the system of nonlinear equations and including a scale factor. The scale factor is such that when adjusted to the unit value, it allows to obtain the solution of the nonlinear equation system. The initial residue is calculated from an estimate to obtain the solution of the nonlinear equation system. In formulating the holomorphic embedding approach, this initial estimate is called "seed solution". Its estimation in turn, in this dissertation, is determined by calculating the solution of the EDP without transmission losses. The holomorphic embedding method used in this dissertation employs a formulation that advocates obtaining a Taylor series with a reduced number of coefficients. The series is then treated and approximated by a rational fraction, called Padé approximant. This is a positive factor, since high degree polynomials tend to have coefficients with very low (high) absolute values. In this case, the search for a solution of the nonlinear equation systems may stagnate at a value far from the solution of interest. Therefore, in case the low-order polynomial solution is insufficiently accurate, a restart process is performed to compute the series coefficients again. However, now, using as seed solution the most updated Padé approximation. The cost optimization process for power generation in the generating units takes into account the operational limits of these variables. The same EDP is solved by the classic Newton-Raphson method. The purpose is to have a computational reference to evaluate the performance of the proposed technique. Computational simulations in three test systems, considering some different loading for each of them, are used as means to evaluate the performance of the PDE solution through the holomorphic embedding technique. The results show that the proposed method presents results similar to those found by the solution with the traditional Newton-Raphson method. The advantage of the proposed technique lies in the fact that a recursive approach is used to determine the Taylor series coefficients and its robustness for determining the solution of the problem as demonstrated by monitoring the solution residues.

Keywords: Economic dispatch, holomorphic embedding, restart, Newton-Raphson method, transmission losses, Taylor series, Padé approximant.

Contents

1	INTRODUCTION	1
1.1	Overview	1
1.2	Motivation of Study	2
1.3	Objectives	3
1.4	Main Contributions	3
1.5	Related Publications	3
1.6	Organization of the Work	5
2	ECONOMIC DISPATCH PROBLEM	6
2.1	Introduction	6
2.2	Economic Dispatch Studies	6
2.3	The Basic Economic Dispatch Aspects	7
2.3.1	Problem Formulation	8
2.3.2	The Classical Lossless EDP	11
2.3.3	The Lossy Transmission Line EDP	11
2.3.4	Lagrangian for a lossless transmission system	14
2.3.5	Lagrangian for a lossy transmission system	15
2.4	Traditional Optimal Solution Methods	17
2.4.1	The Interior Points Method	17
2.4.2	The Reduced Gradient Method	18
2.4.3	The Newton-Based Method	19
2.4.4	The Quadratic Programming Method	20
2.4.5	Comparison of Traditional Models: IPM, RGM, NBM and QP Methods	21
2.4.6	Motivation for Non-Iterative Methods Development	22
2.5	Non-Iterative Methods	22
2.5.1	Motivation for The Holomorphic Embedding Load Flow Method Development	22
2.6	Conclusion of this Chapter	23

3	THE HOLOMORPHIC EMBEDDING METHOD	24
3.1	Introduction	24
3.2	Holomorphic Functions	24
3.3	Power Series Expansion of Holomorphic Functions	25
3.4	Holomorphic Embedding of Nonlinear Equations	26
3.5	Analytic Continuation and Padé Approximants	28
3.6	Matrix Representation of the Taylor Series Coefficients for a General System	29
3.7	Overview of The Holomorphic Embedding Load Flow Method	31
3.8	State of the Art about Some Existing Holomorphic Embedding Method Approaches	31
3.9	Conclusion of this Chapter	33
4	THE HOLOMORPHIC EMBEDDING METHOD USED FOR SOLVING THE ECONOMIC DISPATCH PROBLEM	34
4.1	Introduction	34
4.2	Problem Formulation	34
4.3	The Holomorphic Embedding Method Strategy	37
4.4	The Holomorphic Embedding Model for the EDP	41
4.4.1	Embedding Equations Based on the Residue	43
4.5	Conclusion of this Chapter	48
5	METHODOLOGY AND RESULTS	49
5.1	Introduction	49
5.2	Test System Models	49
5.3	General Aspects of the Numerical Techniques	51
5.4	Experiments and Results	53
5.4.1	System 1	53
5.4.2	System 2	60
5.4.3	System 3	70
5.5	Conclusion of this Chapter	80
6	CONCLUSION	81
6.1	Conclusion	81
6.2	Future Works	82
	BIBLIOGRAPHY	83

List of Tables

5.1	Fuel price in \$/MBTU for the system 1	53
5.2	Heat curve parameters for thermal units in MBTU/h of the system 1	54
5.3	Operational Limits CS, in pu	54
5.4	Economic Dispatch Results System 1 CS	55
5.5	Operational Limits MS	57
5.6	System Loading MS	57
5.7	Economic Dispatch Results System 1 MS	57
5.8	Operating Limits RS	59
5.9	System Loading RS	59
5.10	Economic Dispatch Results System 1 RS	59
5.11	Fuel Cost System 2	61
5.12	Heat Curve Parameters System 2	61
5.13	Operating Limits CS	62
5.14	Economic Dispatch Results System 2 CS	62
5.15	Operating Limits MS	64
5.16	System Loading MS	64
5.17	Economic Dispatch Results System 2 MS	65
5.18	Operating Limits RS	67
5.19	System Loading RS	67
5.20	Economic Dispatch Results System 2 RS	68
5.21	Fuel Cost System 3	70
5.22	Heat Curve Parameters System 3	70
5.23	Operating Limits CS	71
5.24	Economic Dispatch Results System 3 CS	72
5.25	Operating Limits MS	73
5.26	System Loading MS	74
5.27	Economic Dispatch Results System 3 MS	75
5.28	Operating Limits RS	77
5.29	System Loading RS	77
5.30	Economic Dispatch Results System 3 RS	78

List of Figures

2.1	Generation and load aggregated at a bus - a lossless case	11
2.2	System formed by a power generation connected to a transmission line to supply a load P_L	11
3.1	Traditional HEM Flowchart	32
4.1	Restarted HEM Flowchart	43
5.1	3-bus test system schematic	50
5.2	9-bus test system schematic	50
5.3	14-bus test system schematic	51
5.4	Comparative Solution Error System 1 CS	56
5.5	Comparative Solution Error System 1 MS	58
5.6	Comparative Solution Error System 1 RS	60
5.7	Comparative Solution Error System 2 CS	63
5.8	Comparative Solution Error System 2 MS	66
5.9	Comparative Solution Error System 2 RS	69
5.10	Comparative Solution Error System 3 CS	73
5.11	Comparative Solution Error System 3 MS	76
5.12	Comparative Solution Error System 3 RS	79

SYMBOL LIST AND ABBREVIATION

α	Complex variable used in holomorphic embedding
a	Unknown coefficients in the numerator polynomial of the Padé approximant
ANN	Artificial Neural Network
b	Unknown coefficients in the denominator polynomial of the Padé approximant
B	Shunt susceptance(\mathcal{U})
c_i	Unknown coefficients in the fuel cost
CS	Conservative Scenario
DED	Dynamic Economic Dispatch
DP	Dynamic Programming
ξ	Solution Error
ED	Economic Dispatch
EDP	Economic Dispatch Problem
F_i	Cost Function for Machine i
f_{1i}	Unknown coefficients in the cost function
f_{2i}	Unknown coefficients in the cost function
f_{3i}	Unknown coefficients in the cost function
G	Conductance (\mathcal{U})
GSA	Gravitational Search Algorithm
h_{1i}	Unknown coefficients in the heat curve
h_{2i}	Unknown coefficients in the heat curve
h_{3i}	Unknown coefficients in the heat curve
HE	Holomorphic Embedding
HEM	Holomorphic Embedding Method
IPM	Interior Points Method

\mathbf{J}^k	Jacobian Matrix
KKT	Karush-Kuhn-Tucker Optimal Conditions
λ_i	Marginal Cost Variable
L	Degree of numerator polynomial in the Padé approximant
LF	Lagrangian Function
μ_i	Relaxation Parameter
M	Degree of denominator polynomial in the Padé approximant
MS	Moderate Scenario
\mathbf{R}^k	Mismatch Vector
N	Number of Generating Units at bus i
NB	Number of Buses
NBM	Newton-Based Methods
NG	Number of Generating Units
OF	Objective Function
π	Slack Cost Variable
P_i	Power Output at bus i
\underline{P}_i	Lower Power Output Limit at bus i
\overline{P}_i	Upper Power Output Limit at bus i
P_{FL}	Load Flow at bus i
P_{Load}	Load connected at bus i
P_{Losses}	Losses connected at bus i
P_k	Dependent Generator Power output
PSO	Particle Swarm Optimization
pu	<i>Per Unit</i>
QP	Quadratic Programming
r	Unknown Quadratic Coefficient
RS	Radical Scenario
s	Unknown Linear Coefficient
SED	Static Economic Dispatch
SGM	Sub-Gradient Method
θ_i	Voltage angle at bus i
t	Unknown Constant Coefficient
u	Unknown Linear Coefficient
UC	Unit Commitment
UCP	Unit Commitment Problem

v	Unknown Constant Coefficient
$x(\alpha)$	Unknown function of α
Y	Transmission Line Admittance (\mathcal{U})
Y_{bus}	Bus admittance matrix
Y_{ik}	Admittance bus matrix entry between bus i and bus k
Z	Transmission Line Impedance (Ω)

Chapter 1 INTRODUCTION

1.1 Overview

The Economic Dispatch Problem (EDP) in power systems is still up to today an extensively studied topic. The importance of the EDP originates due to the constant need for an optimal energy management. Every power system operator has to manage information which is useful for optimizing resources used in the system. An important aspect taken into account is the power dispatch involving the several power generation units available in the system. In this sense, it is important to determine the power output for every machine that can be under control. The economic dispatch of generation units is useful to plan the daily power output or a more timely output such as hourly. This time dependent solution is what differs the Dynamic Economic Dispatch Problem (DEDP) from the conventional EDP. The more accurate the hourly-interval, the less computational demanding, and with more manners to individualize for its users application the better.

Several different methods are investigated in the search for a more efficient or faster solution, especially for the DEDP. Nowadays, it is possible to find many methods for solving a number of different configurations of the EDP and DEDP like the ones proposed in [1–3]. When transmission losses are included in the problem formulation, a nonlinear system needs to be solved to satisfy these constrains. The challenge is to employ an adequate method to determine the optimal solution for the problem. Among the approaches, there are the ones based on the Newton method, genetic algorithm, interior points method and several hybrid techniques that combine different approaches in the attempt to minimize the originals downsides [4–8]. However, each technique and configuration presents its owns pros and cons. In the line of innovative thinking the Holomorphic Embedding Method (HEM) is a design that must be explored concerning its prospects for improved solution accuracy.

The HEM was originaly proposed to solve nonlinear systems as those ones arising in the power flow problem in power systems [9, 10]. By this technique, a system of nonlinear equations are embedded as a function of a scaling factor in such way that

the result of interest occurs when the scaling factor is adjusted to the unitary value. The solution of the problem is determined in two main steps: firstly, it is computed a finite Taylor's power series for each variable of the nonlinear system as a function of the scaling factor. In the sequence, the power series is converted to into a rational fraction called Padé approximant. There are many ways to embed the problem and obtain the solution of the nonlinear system by applying the HEM. In [9], it is calculated a power series, in general with an elevated number of coefficients. The elevated polynomial orders generate very high (or very low) coefficient values, which required improvement in terms of accuracy (above double-precision accuracy) for handling such coefficients. In [11], the problem of elevated order for the power series was circumvented, by using a strategy that takes into account an initial guess and a restart process.

1.2 Motivation of Study

Inspired on the use of the HEM applied to solve the nonlinear problem of the load flow in power systems, the idea is to investigate the EDP considering the HEM to find the solution associated to the nonlinear problem. Some aspects are commented about the HEM recent application.

The Holomorphic Embedding method (HEM) is a method based on the technique of complex analysis. The technique was first proposed in power systems recently by Trias [9]. And later on modified by others for a better response [12], or smaller order coefficients [11].

The HEM exploits the technique of complex embedding to convert the problem's modeling functions to be holomorphic functions. The power dispatch for each unit and the marginal prices solution is represented by the Padé approximants, which is a set of rational equations obtained from the MacLaurin series expansion of the holomorphic functions.

This method requires no initial value estimate, though it does require a *germ solution* which can be found by a linear system solution. The HEM eliminates the uncertainty of solution existence faced by all iterative solution methods. It is guaranteed to converge if it has a solution, and unequivocally signals when no solution exists. Furthermore, it can guarantee convergence, even though with precision issues [9], [12].

The HEM is a good candidate for solving EDP because of its high reliability. To this point, the literature contains no reports that the algorithm has been tested for solving economic dispatch problems, only for power flow problems.

1.3 Objectives

The objectives for this dissertation are two: adapt and test the Holomorphic Method proposed by [11] as a solution algorithm for the Economic Dispatch with transmission losses, and investigate its robustness, reliability and accuracy when compared with the traditional Newton-Raphson method for solving nonlinear equation systems.

1.4 Main Contributions

This dissertation investigates the application of the Holomorphic Embedding Method for Solving the Economic Dispatch for Thermal units under a lossy transmission system. It can highlight as contributions the following aspects:

- The similar accuracy of the method when compared with the traditional Newton-Raphson method;
- The smaller dependency on the initial guess or *germ solution* as the iterative methods available;
- The restarted approach that reduced the order of the Taylor series and Padé rational equations.

1.5 Related Publications

There are some interesting works related to the Economic Dispatch Problem and the Holomorphic Embedding method that were used as research on this dissertation. Regarding the Holomorphic Embedding method the succeeding references can be mentioned:

- The paper [9] by Antonio Trias is the initial study on the new method and laid the foundation for developing the method employed in this dissertation;
- The method developed in [11] was the chosen one as the base for this work. It uses a restarted approach with a very reduced number of coefficients;
- Shukla in [13] applies the Holomorphic method to the Unit Commitment problem in order to calculate the load flow within;
- Again in [7] the Unit Commitment problem uses the holomorphic method as part of the solution associated with the Gravitational Search algorithm;
- Finally in [14] it is presented a new type of problem, the Voltage Stability, is also solved via Holomorphic Embedding method.

As far as the important works related to the Economic Dispatch is important to mention the ones addressing the differences in the problem modeling, the several algorithms available for solution as well as the most recent developments. These can be found bellow.

- Recently new aspects of the Economic dispatch modeling are at evidence, [15] for instance investigate what are the impacts of implementing penalty factors;
- Fadil in [16] investigated differences in modeling of the EDP by including among the restrictions prohibited operating zones for the thermal machines;
- Sydulu in [3] used a different model for the fuel cost, applying a cubic function to cater for the dependency of the output to the constitutive parameters of a thermal machine;
- It is also interesting to highlight the work of Han in [17] since it is studied a variation of EDP where the problem takes into account the loading change throughout time;
- Lastly paper [18] set the foundation for the dynamic lossy EDP with early studies on the matter.

1.6 Organization of the Work

This dissertation is organized in the following manner:

- Chapter 2 discuss the Economic Dispatch Problem, its characteristics and some traditional solution methods;
- Chapter 3 explains the Holomorphic Embedding method and present generic equations for the problem;
- Chapter 4 examines the economic dispatch using the holomorphic embedding method presenting the main technique used in this dissertation;
- Chapter 5 exposes the numerical results, for the economic dispatch solved via holomorphic embedding, for the selected cases and scenarios;
- Chapter 6 is the conclusion of this dissertation, where the final aspects are presented and future works suggested.

Chapter 2 ECONOMIC DISPATCH PROBLEM

2.1 Introduction

This chapter presents the basic model for the general economic dispatch problem and some adopted solution methodologies. Firstly, it is presented the problem aspects, modeling and related variables. Subsequently, the traditional techniques used for the problem solution is mentioned. Then, these conventional methods are compared and it is introduced the motivation to use the the non iterative model for solving the EDP, called Holomorphic Embedding Method applied to EDP.

2.2 Economic Dispatch Studies

Economic dispatch studies are undertaken for various reasons, some of which are the following [17] [19]:

- Reduction of costs for energy generation;
- Reduction of technical losses;
- Increase in the power plants efficiency;
- Increase of the power plants operators return;
- Improvement in power plant operation due to the increase of renewable energy sources;
- Improvement of system's assets operation.

2.3 The Basic Economic Dispatch Aspects

The EDP is traditionally formulated as the minimization of an objective function based on the costs associated with the generation from hydro and/or thermal power plants [20]. However, this is a more open denomination for a set of problems that are very distinct from one another. Within this denomination there are the Static Economic Dispatch (SED) and the Dynamic Economic Dispatch (DED), both of them can either have a lossless or lossy transmission lines [18].

When the transmission losses are considered the EDP becomes a nonlinear problem. Even though there are several ways to model the losses such as via B-Matrix [20], via quadratic loss curve associated with the generation [21] and via linear load flow [16], only the later is the one being used in this dissertation.

There are several differences between SED and DED, a very important one is how the load is treated. For example, in the SED the load is considered fixed throughout the stipulated time interval whereas for the DED the load varies along the same period of time. The variation of load in the DED can be within minutes, hours, days, etc. This frequency is defined by what are the problem's needs. The same reason is valid for stipulation of the complete time interval of the DED and SED as well.

Other characteristics that can be used for distinction among the different EDPs are for instance the use of penalty factors like the ones used in [15] or the use of ramping rate as in [22], [17]. There is also the use of environmental cost as one of the problem's constraints like in [7] as well as the use of maintenance costs also applied in [7]. Although, the latter is more commonly found in Unit Commitment (UC) problems, which is a similar problem to the Economic Dispatch.

These are some examples on how the EDP formulation can be diverse. Nonetheless, this dissertation is focused only in SED without penalty factors, environmental and maintenance costs or ramping rates, in a lossy transmission system.

2.3.1 Problem Formulation

This dissertation's proposed SED problem is formulated around the following guidelines:

- Only thermal generators are used in the system;
- The transmission line losses are modelled by a quadratic function which is a function of only the voltage phase angle; therefore, voltage magnitude at each bus is assumed equal to 1.0 pu;
- Each thermal unit has its own heat curve and fuel price;
- Each thermal unit has its own operational limits;
- No constraints regarding the transmission lines capacity;
- No maintenance or environmental costs are considered;
- Every bus can be at the same time generating and consuming power.

The first one ensures a homogeneous system. The following was chosen based on the suitability of its mathematical function for holomorphic embedding transformation. The third and fourth allow a more real representation of the power system singularity. No maintenance or environmental costs were considered since down times or natural impact were not within of the objectives of this work. At last longing for a more flexible and close to reality like system configuration, all buses can be either for generation, consumption or both.

With these rules the problem is modelled in the following order:

- Cost functions definition;
- Constraint functions determination;
- Objective function formulation;
- Lagrangian function construction;
- Optimality conditions estimation.

2.3.1.1 Cost Functions

The costs function, $F_i(P_i)$, is the mathematical function used to emulate the costs for a specific generating unit i for a certain amount of power output P_i . This function is obtained by multiplying the fuel price c_i U\$ by the generating unit heat curve $H_i(P_i)$ in BTU. The generator's heat curve is a function that depends on its mechanical, electrical and external characteristics.

This curve can be formulated in several different ways such as quadratic functions [6], cubic functions [3] or like in [21] as a polynomial function. The most commonly found is the first one, that will also be the formulation adopted in this dissertation.

$$H_i = h_{1i}P_i^2 + h_{2i}P_i + h_{3i} \quad (2.1)$$

$$F_i(P_i) = c_i H_i(P_i) \quad (2.2)$$

$$F_i(P_i) = f_{1i}P_i^2 + f_{2i}P_i + f_{3i} \quad (2.3)$$

The parameters h_{1i} , h_{2i} and h_{3i} are different for each curve and are the ones determined by the machines characteristics. However, they are constant. The parameter c_i is the fuel price and depends only on the type of fuel being used on the machine and market conditions. Although the fuel price may varies for each scenario it will be a fixed value that will not change throughout the simulation. Thus f_{1i} , f_{2i} and f_{3i} will remain as constant values for each simulation.

2.3.1.2 System's Constraints formulation

The constraints can be divided into two categories, equality constraints and inequality constraints. The first one accounts for the system's power balance and also spinning reserve, if the problem considers these to be part of its model. The second one caters for all the rest of the problem's considerations, such as:

- Machine's operating limits;
- Maintenance costs;
- Environmental costs;

- Transmission lines capacity;
- Prohibited operating zones.

The equality constraints need no special manipulation in order to be inserted in the Lagrangian function whereas the inequality ones need. The inequality constraints must first be separated into two equations whenever there are an upper and lower limits. Then one of these "new" inequalities constraints is used for each type of violation, upper or lower.

Considering NG thermal units connected at a bus and a transmission system, the equality constraint is of the type:

$$\sum_{i=1}^{NG} P_i = P_{Load} + P_{Losses} \quad (2.4)$$

or as

$$\sum_{i=1}^{NG} P_i - P_{Load} - P_{Losses} = 0 \quad (2.5)$$

where P_i is the power generation of unit i , NG is the number of generating units, P_{Load} is the load and P_{Losses} represents the loss term.

The inequalities are attributed only to the power generation units. They are of the form:

$$\underline{P}_i \leq P_i \leq \overline{P}_i \quad (2.6)$$

also separated as two single-limit inequalities

$$\underline{P}_i - P_i \leq 0, \quad P_i - \overline{P}_i \leq 0 \quad (2.7)$$

where \overline{P}_i and \underline{P}_i are respectively the upper and lower machine's operating limits units.

On equation (2.4) it is shown the equality constraint for the system's power balance. In (2.6) it is portrayed the generating units operating limits, which is the only inequality constraint considered for this dissertation. Expressions in (2.7) shows the process for dissociation into two inequalities constraints.

2.3.2 The Classical Lossless EDP

The classical lossless EDP is presented in [20] when the term P_{Losses} is neglected in (2.4). For this formulation the power generation and load are aggregated at the own bus. The diagram in Figure 2.1 illustrates this situation.

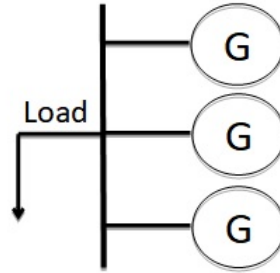


Figure 2.1: Generation and load aggregated at a bus - a lossless case

2.3.3 The Lossy Transmission Line EDP

The transmission line loss term P_{Losses} in (2.4) is referred to as the total losses in all interconnection $i - j$ of the network. The loss at a given interconnection circuit $i - j$ is calculated considering the power flowing from the bus i to j . This is a nonlinear term. The reference [20] presents an example for two buses, where one bus has a power generation and another bus has only a load P_L (see Figure 2.2 for details).

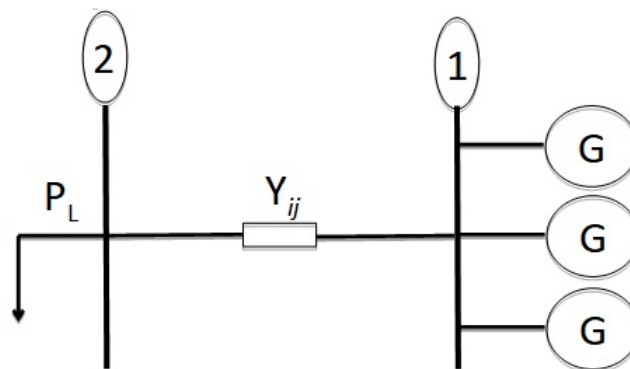


Figure 2.2: System formed by a power generation connected to a transmission line to supply a load P_L

In general, simplifications are assumed for the lossy EDP. In [20] for the 2-bus system, the losses in the interconnection transmission line are calculated as a quadratic

function of the output power supplied by the units connected to the bus 1. In [1], a multibus system is studied. In this work, the transmission network loss is a function of the output real power of thermal generation units and is given by (2.8):

$$P_{Losses} = \sum_{i=1}^{NG} \sum_{j=1}^{NG} P_i B_{ij} P_j \quad (2.8)$$

where B_{ij} are known as the loss coefficients or B-coefficients.

As in the 2-bus case, the losses in the multi-bus case also depend only of the unit output power and the B-coefficients. The computation of these coefficients assumes that the system is operating on a given point (see [23] for details). However, the economic dispatch is just a procedure to determine the power dispatch in order to achieve the lowest cost. Therefore, on adopting the B-coefficients method the computation of the coefficients is verified for an operation point. Then, for a different operation point this result can present significantly different characteristics.

Another method considers the active power flow from a bus i to j , P_{Dij} . By this technique, the loss between two interconnected buses is calculated as $P_{loss}^{ij} = P_{Dij} + P_{Dji}$. The active power flow is approximated by [24]:

$$P_{Dij} = -b_{ij}\theta_{ij} + \frac{1}{2}g_{ij}\theta_{ij}^2 \quad (2.9)$$

where $\theta_{ij} = \theta_i - \theta_j$ and $y_{ij} = g_{ij} + jb_{ij}$ is the connecting (series) admittance between the two buses i and j .

Therefore, the loss in the interconnection $i - j$ is $g_{ij}\theta_{ij}^2$.

The total power flow in the network is

$$P_{FL} = \sum_{ij \in \Omega}^{N_{int}} [-b_{il}(\theta_i - \theta_j) + \frac{1}{2}g_{ij}(\theta_i - \theta_j)^2] \quad (2.10)$$

where Ω represents the set of interconnections in the system and N_{int} is the total number of interconnection ij for the system.

Since each bus i may be connected through multiple lines to several buses j the total load flow P_{FL} are the sum of the load flows in all the lines connecting two buses in the system.

Differently from the method based on the B-coefficients for computation of loss, expression (2.10) depends on the parameters of the interconnection and the phase angles at the two terminals of the circuit. In view of these details, this modelling presents a physical aspect more appropriated to model the loss. Then, the loss representation (2.9) will be the option used to model the loss in a transmission line in this work.

2.3.3.1 Objective Function Formulation

The Objective Function (OF) is the function that specifies what will be maximized or minimized by the Lagrangian function. In the case of EDP the primal interest is to minimize the costs for generating power. However other goals might be of concern such as minimization of losses, minimization of lines loading, etc. As mentioned before, this work is interested only in the primal objective. Thus the OF will portray only the reduction of generation costs. Then, the OF is defined as

$$\text{Min} \sum_{i=1}^{NG} F_i(P_i) \quad (2.11)$$

for all NG generation unit in the network

Case there is more than one objective for the EDP, for instance the minimization of costs and losses simultaneously. This double objective will be reflected in the OF. In this case the OF will have more than one equation. For the example described above the OF will be minimum of the costs sum and the minimum of the losses sum. This can be extended for any number of objectives. Each new objective added to the problem will result in a new function added to the OF.

2.3.3.2 System's Lagrangian Function

The Lagrangian Function (LF) is the mathematical model that ties together all elements of the EDP, the constraints and the objective function. When formulating the LF it is also added the marginal cost variable or Lagrangian multipliers, λ_i , and the lagrange multiplier for machines that are operating above or below its limits, π_i . The LF is constructed following this steps:

- Initialize by the objective function;
- Multiply each equality constraint by a marginal cost variable λ_i ;
- Subtract each of the above products from the objective function;
- Multiply each inequality constraint by a lagrange multiplier π_i ;
- Add each of the above products to the objective function with the equality constraints;
- The objective function minus the equalities constraints product added to the inequalities constraints product is the LF.

2.3.4 Lagrangian for a lossless transmission system

Suppose a N_b -bus system supplied by thermal units. The units are connected to N_g buses and each bus i has N_{gi} units. Each bus $\ell = 1, \dots, N_b$, including generation buses, has an aggregated load $P_{L\ell}$. For this problem, the lossless EDP can be stated as

$$\begin{aligned}
 LF(P, \lambda, \pi) = & \sum_{i=1, i \in \Omega_g}^{N_g} \sum_{j=1}^{N_{gi}} F_{ij}(P_{ij}) - \sum_{\ell=1}^{N_b} \lambda_{\ell} \left[\left(\sum_{j=1, \ell \in \Omega_g}^{N_{g\ell}} P_{\ell j} \right) - P_{L\ell} \right] + \\
 & + \sum_{i=1, i \in \Omega_g}^{N_{bg}} \sum_{j=1}^{N_{gi}} \underline{\pi}_{ij} (\underline{P}_{ij} - P_{ij}) + \sum_{i=1, i \in \Omega_g}^{N_{bg}} \sum_{j=1}^{N_{gi}} \bar{\pi}_{ij} (P_{ij} - \bar{P}_{ij}) \quad (2.12)
 \end{aligned}$$

where N_{bg} is the number of generation buses in the system; N_b is the the total number of system bus; N_{gi} is the number of generation buses connected to the bus i ; Ω_g is the set of bus generation; $F_{ij}(P_{ij})$ is the cost function associated to the unit j which is connected to the generation bus i ; P_{ij} is the power output of the unit j connected to the bus i ; λ_{ℓ} is the Lagrange multiplier associated to the system bus ℓ ; $P_{L\ell}$ is the aggregated load connected to the bus ℓ ; $\underline{\pi}_{ij}$ and $\bar{\pi}_{ij}$ are the lagrange multipliers for the lower and upper limits related to violation on P_{ij} , respectively; \underline{P}_{ij} and \bar{P}_{ij} are the lower and upper limits established for P_{ij} , respectively.

In the next subsection, the Lagrangian for a lossy transmission system is introduced.

2.3.5 Lagrangian for a lossy transmission system

The Lagrangian function for a lossy transmission system is given by

$$\begin{aligned}
LF(P, \lambda, \pi) = & \sum_{i=1, i \in \Omega_g}^{N_g} \sum_{j=1}^{N_{gi}} F_{ij}(P_{ij}) - \sum_{\ell=1}^{N_b} \lambda_{\ell} \left[\sum_{j=1, \ell \in \Omega_g}^{N_{g\ell}} P_{\ell j} - P_{L\ell} - \sum_{j \in \Omega_{\ell}} P_{D\ell j} \right] + \\
& + \sum_{i=1, i \in \Omega_g}^{N_g} \sum_{j=1}^{N_{gi}} \pi_{ij} (P_{ij} - \underline{P}_{ij}) + \sum_{i=1, i \in \Omega_g}^{N_g} \sum_{j=1}^{N_{gi}} \bar{\pi}_{ij} (P_{ij} - \bar{P}_{ij}) \quad (2.13)
\end{aligned}$$

where here $P_{D\ell j}$ is the active power flow flowing from the bus ℓ to j Ω_{ℓ} is a set of buses that has connection with the bus ℓ .

Analyzing the variables in the LF formulation, two sets of them have an economical meaning and distinct understanding: λ_i and π_i . The variable λ_{ℓ} is the marginal cost associated with the system bus ℓ . This means that a positive value translates into the more power is generated in the bus the cheaper will be the total cost, and a negative value is the opposite the more load or losses associated with the bus the more expensive will be energy cost. Thus a negative value for any of the λ_i is not desirable.

The analysis for the other economic parameter π_{ij} , the lagrange multiplier, is a bit different. A positive value for π_{ij} indicates that constraint associated with the violating unit is valid and therefore must be kept. This entails in a different marginal cost for the violating unit. This unit marginal cost will no longer be the λ_i associated to its bus, it now will be the lagrange multiplier plus the bus λ_i value. In the case of a negative π_i value, the constraint must be removed from the LF. Because, it is not economically valid any more since it incurs in an elevation of cost. Whenever there is a negative lagrange multiplier, this variable must be removed from the system and the values must be recalculated.

The variables in the LF may vary according to the OF and constraints considered for the EDP. However, they will be always characterized by three very distinct set of equations. The first set are the equations that constitutes the OF, this set has no additional variable associated with it. The second set is formed by the equations that constitutes the equalities constraints, they are characterized by their association to a marginal price variable (λ_i). Finally the third set are the equations arisen from the inequalities constraints, they will have a lagrange multiplier (π_i) associated with it.

2.3.5.1 Optimality Conditions

The optimality conditions are all derived from the LF, they are the so called Karush-Kuhn-Tucker (KKT) conditions. These conditions will form the equations system that need to be solved in order to calculate the EDP solution for a given system in a specific period of time.

The KKT conditions are the first partial derivative of the LF in respect to the generators power (P_{ij}), in respect to the incremental costs (λ_ℓ), in respect to the voltage phases θ_m , and in respect to the lagrange multipliers ($\underline{\pi}_{ij}, \bar{\pi}_{ij}$). This set of equations form a nonlinear system that must be solved in order to calculate the power generation, incremental costs for each unit and in case of operating limit violation the lagrangian multiplier associated with the violating power generation. This system can be represented by the following equation set:

$$\frac{\partial LF}{\partial P_{ij}} = \frac{\partial F_{ij}}{\partial P_{ij}} - \lambda_i + \bar{\pi}_{ij} - \underline{\pi}_{ij} = 0, \quad i = 1, \dots, N_{bg}, \quad j = 1, \dots, N_{gi} \quad (2.14)$$

$$\frac{\partial LF}{\partial \lambda_\ell} = - \left[\sum_{j=1, \ell \in \Omega_g}^{N_{g\ell}} P_{\ell j} - P_{L\ell} - \sum_{j \in \Omega_\ell} P_{D\ell j} \right] = 0, \quad \ell = 1, \dots, N_b \quad (2.15)$$

$$\frac{\partial LF}{\partial \theta_\ell} = \frac{\partial \left\{ \sum_{\ell=1}^{N_b} \lambda_\ell \left[\sum_{j \in \Omega_\ell} P_{D\ell j} \right] \right\}}{\partial \theta_\ell}, \quad \ell = 2, \dots, N_b \quad (2.16)$$

$$\frac{\partial LF}{\partial \bar{\pi}_{ij}} = (P_{ij} - \bar{P}_{ij}) = 0, \quad i = 1, \dots, N_{bg}, \quad j = 1, \dots, N_{gi} \quad (2.17)$$

$$\frac{\partial LF}{\partial \underline{\pi}_{ij}} = (-P_{ij} + \underline{P}_{ij}) = 0, \quad i = 1, \dots, N_{bg}, \quad j = 1, \dots, N_{gi} \quad (2.18)$$

The optimality conditions are the equations that are responsible for finding the minimum/maximum local and global points for the systems functions. Their solution guaranties that the optimal result for all the equations was found.

2.4 Traditional Optimal Solution Methods

Currently, there are many methods for solving the EDP, each one exploiting a specific approach. There are the already established ones like the Reduced gradient Method (RGM) [6, 16], the Newton-Based Methods (NBM) [20], the Interior Points Method (IPM) [5]. There are also the new heuristic based ones like Artificial Neural Network (ANN) [8], Particle Swarm Optimization (PSO) [4] and Gravitational Search Algorithm (GSA) [7] and the ones in between such as the hybrid methods like Multi Gradient PSO [1] and the established but not that widely applied like Dynamic Programming (DP) [18] and Quadratic Programming (QP) [2]. In the following subsection some of these methods are highlighted and compared one another.

2.4.1 The Interior Points Method

The Interior Points Method (IPM) is a widely applied solution method for ED [5, 26]. It consists on a solution method that obtains the optimum solution by moving the evaluation plane and narrowing the feasible space that is surrounded by the evaluation plane and the constraints planes.

When modelling the inequality constraints the IPM in order to contour the problem of non-convergence of the solutions due to harsh restrictions, it is introduced a new parameter (μ_i) that loosens the complementary constraints allowing this way a more smooth convergence for the equations.

The LF for the IPM is the same as any other method, and from it are derived the optimality conditions. The difference comes in the optimality conditions originated from the inequalities constraints. On these equations the parameter (μ_i) is introduced in the equation in order to wide the convergence plane for the equation, since the original one is very narrow and depending on the initial guess might not converge. Thus the system of optimality conditions equations is represented by (2.19), (2.20), (2.21) and (2.22)

$$\frac{\partial LF}{\partial P_{ij}} = \frac{\partial F_{ij}}{\partial P_{ij}} - \lambda_i \pm \pi_{ij} = 0, \quad i = 1, \dots, N_g, \quad j = 1, \dots, N_{gi} \quad (2.19)$$

$$\frac{\partial LF}{\partial \lambda_i} = \sum_{ij \in \Omega} P_{Losses}^{ij} + P_{Li} - \sum_{i=1}^{N_g} \sum_{j=1}^{N_{gi}} P_{ij} = 0 \quad (2.20)$$

$$\frac{\partial LF}{\partial \bar{\pi}_{ij}} = (P_{ij} - \bar{P}_{ij})\pi_{ij} = \bar{\mu}_{ij} \quad (2.21)$$

$$\frac{\partial LF}{\partial \underline{\pi}_{ij}} = (-P_{ij} + \underline{P}_{ij})\pi_{ij} = \underline{\mu}_{ij} \quad (2.22)$$

In order to return to the original problem the variable introduced for the constraints relaxation (μ_{ij}) must be reduced to zero. This is done by updating the variable's value and using the previous solution to the problem in order to calculate another one for the new μ_i value in an iterative way, until the value of μ_{ij} is within an accepted margin of zero.

The nonlinear system composed by set of modified optimality conditions is solved by Newton-Raphson, this being the reason why this solution method might encounter some convergence issues even with the introduction of the relaxation parameter.

2.4.2 The Reduced Gradient Method

The Reduced Gradient Method (RGM) also known as the Reduced-Gradient Method or as Reduced-Hessian Method takes advantage of the existing relation between the system's variables due to the equality constraints. This means that there will be dependent variables and independent variables for the generators power output. The dependent variables originated from the equality constraints, one for each constraint, will cause a reduction in the size of the jacobian matrix, thus originating a more fast and less computational burdening solution.

The first step is to chose which generator will be the dependent one (P_k), one for each equality constraint, then its power equation must be rewritten accordingly, as a function of the rest of the generators (P_i) power's equations as depicted in (2.23):

$$P_k = P_{Load} - \sum_{i \neq k}^N P_i \quad (2.23)$$

With the dependable variables selected and its equations defined, the initial values for the control variables (P_i) must be defined. They must be within the system's operational limits so the π_i variables are all equal to zero. From the P_i it is calculated the P_k values using (2.23). In order to calculate the λ_i values for the initial guess values, the partial derivative from the control variables must be calculated.

Then the reduced gradient is calculated only with the control variables. From the reduced gradient it is possible to determine whether the initial guess must be lowered or increased depending if the greater value is positive or negative.

From the values of the reduced gradient the cost must be calculated from the problem's formulating equations. The cost variation is obtained through (2.24). This process must be repeated until the variation between the calculated costs are within the accepted limits.

$$\Delta F(\mathbf{P}) = \nabla F(\mathbf{P})^t \cdot \Delta \mathbf{P} \quad (2.24)$$

2.4.3 The Newton-Based Method

The Newton-Based Methods (NBM) are already a traditional approach solving the EDP. They consist in simply solving the nonlinear equation system formed by the first derivative of LF, the optimality conditions, via Newton-Raphson approach. No adaptation for the equations is used like in the SBM and no other variables are introduced like in the IPM.

The primary step for this method is an initial guess (P_{ij}^0 and λ_i^0) for the variables P_{ij} and λ_i , this guess will be such that no power limits are violated therefore, all π_{ij} are equal zero and the system is composed only of the equations (2.14) and (2.15). Since the NBM are highly dependent on the initial guess, a good one for the lossy system is the solution for the lossless system. Once the initial guess was defined the solution is executed by the following algorithm:

1. Make $k = 0$;
2. Calculate the mismatch vector \mathbf{R}^k ;

3. Calculate the Jacobian Matrix \mathbf{J}^k ;
4. Calculate the incremental value for the variables as shown in (2.25);

$$[\Delta P_{ij}^{(k+1)T} \quad \Delta \lambda_i^{(k+1)T}]^T = -\mathbf{J}^k \mathbf{R}^k \quad (2.25)$$

5. Calculate the new values for the variables by (2.26);

$$P_{ij}^{k+1} = P_{ij}^k + \Delta P_{ij}^{k+1}, \lambda_i^{k+1} = \lambda_i^k + \Delta \lambda_i^{k+1} \quad (2.26)$$

6. Make $k = k + 1$;
7. Calculate the error (ξ) for the new values of the variables;
8. If the error ξ is not within the accepted convergence ratio resume to step 2, otherwise P_{ij}^{k+1} and λ_i^{k+1} are the EDP results.

If no variable exceeds the operating limits this will be the problem solution, in case any of the variables exceeds its limits you must set the exceeding variable to its limit, and add the constraint equation related to the exceeded limit to the nonlinear system. Once this equation has been added you will follow once more the algorithm for the new system solution. This must be done for every machine that is operating outside its limits.

2.4.4 The Quadratic Programming Method

The Quadratic Programming (QP) is a method used for solving problems with quadratic objective function and linear constraints. Therefore, it is good fit for the lossless EDP. When is used for solving a lossy EDP the problem's constraints must be adapted to a linear form in order to apply for this method.

This method consists in finding a vector x that minimizes the quadratic function (2.27) subject to a linear inequality (2.28), (2.29) and bound constraint (2.30).

$$\min_x \left(\frac{1}{2} \mathbf{x}^T H \mathbf{x} + f' \mathbf{x} \right) \quad (2.27)$$

$$A \mathbf{x} \leq b \quad (2.28)$$

$$A_{eq} \mathbf{x} \leq b_{eq} \quad (2.29)$$

$$lb \leq \mathbf{x} \leq ub \quad (2.30)$$

This is also an iterative process, hence the vector x must be calculated and updated multiple times until a tolerance value is reached. Unlike most processes this method does not require the construction of a Lagrangean Function then no values for incremental cost λ_i are calculated and no derivatives and optimality conditions are necessary. Since no derivatives are used this method will find a global minimum for the problem.

2.4.5 Comparison of Traditional Models: IPM, RGM, NBM and QP Methods

Some of the comparisons that can be made among the traditional solution methods are:

- QP is the only method capable of finding a global minimum value for the problem, while IPM, NBM and RGM are only capable of finding local minimum solutions. This is due to the fact the QP transforms the problem in a convex problem while the rest does not.
- QP is also the only technique that does not employ the actual system, since a linearization of constraints is due for the algorithm execution, whereas none of the other methods must approximate the conditions;
- IPM and RGM employ the Newton-Raphson for solving the equation system, however, they both developed mechanisms (relaxation parameter, and smaller gradient matrix) for improving the solution, by making it faster more accurate and less computationally burdening;
- IPM also has another advantage when compared to NBM, the relaxation parameter since it prevents the solution from zigzagging enables a better chance of convergence for heavily loaded systems. As the μ_i is introduced the feasible solutions curve becomes more smooth and employs better initial guesses;
- RGM for presenting a reduced gradient when compared to NBM has an advantage of requiring the computation of a smaller number of parameters via iterative manner, causing thus to be less computationally burdening.

All the presented methods have one thing in common though, an iterative component for its solution. Be it the succession of calculations for the \mathbf{x} vector in the QP or the calculation of non-linear constraints systems in the IPM, or repetitively update of the gradient in the RGM or finally by the traditional calculation of the Jacobian matrix and mismatch vector for the NBM.

2.4.6 Motivation for Non-Iterative Methods Development

The traditional solving methods for the EDP work well for a system with few generators, as the number of power units rise their efficiency reduces. This is due to several reasons such as: complexity of the Jacobian matrix for the NBM and RGM; the complexity of the restrictions is a set back for the QP; and the high amount of new variables that are introduced for each generating unit is a red light for the IPM. Furthermore, these iterative methods need an appropriate guess of the initial values. Taking into account these limitations for the traditional methods, non-iterative solutions have been proposed and are yet to be more thoroughly tested [25].

2.5 Non-Iterative Methods

The traditional iterative solution methods are proven to come short when there is a bad initial guess or when there are way to many variables resulting in a singular Jacobian matrix that cannot be inverted, so new non-iterative methods have been studied. Among the non-iterative ways to solve the EDP the Holomorphic Embedding proposed by [9] and latter on improved by [11, 12] was successful in solving the Load Flow problem and will be tested in this dissertation as a way to solve the EDP as well.

2.5.1 Motivation for The Holomorphic Embedding Load Flow Method Development

The Holomorphic Embedding method (HEM) is the most recently developed method based on the technique of complex analysis. The algorithm was first proposed by Trias [9]. And later on modified by others for a better response [12], or smaller order coefficients [11].

The HEM exploits the technique of complex embedding to convert the problem's modelling functions to be holomorphic functions. The power dispatch for each unit and the marginal prices solution is represented by the Padé approximants, which is a set of rational equations obtained from the MacLaurin series expansion of the holomorphic functions.

This method requires no initial value estimate, though it does require a *germ solution* which can be found by a linear system solution. The HEM eliminates the uncertainty of solution existence faced by all iterative solution methods. It is guaranteed to converge if it has a solution, and unequivocally signals when no solution exists. Furthermore, it can guarantee convergence, even though with precision issues [9], [12].

The HEM is a promising candidate for solving the EDP because of its high reliability, though it requires a longer execution time when compared to other EDP algorithms. To this point as far as the knowledge of the author goes, the literature contains no reports that the algorithm has been tested for solving economic dispatch problems, only for power flow problems.

Details of this method will be better explained in Chapter 3.

2.6 Conclusion of this Chapter

In this chapter was introduced four conventional methods (the QP, the NBM, the RGM and the IPM) and discussed about a non-iterative methods (HEM). The conventional methods have a good and reliable performance when dealing with smaller systems and well placed initial guesses, thus this dependency upon the initial values for convergence reduces their applicability. Non-iterative methods are claimed to have improvements regarding the convergence issues and other advantages. As they are much less researched than the conventional methods, they beg adequate study and are open to further developments.

Chapter 3 THE HOLOMORPHIC EMBEDDING METHOD

3.1 Introduction

In this chapter, the Holomorphic Embedding Method is detailed. This methodology is based on the complex analysis and aims to find a solution in a recursive way rather than the iterative.

The method has already been applied [9] to the nonlinear power flow problem with the proper models for load buses (PQ), Generator buses (PV) and *slack* bus, and later on [11], where a restarted approach was developed. Guaranteeing thus its efficiency, as long as the equations describing the power flow are holomorphic embedded, which is done with the inclusion of a complex scaling factor α .

The analytical properties of the holomorphic functions are used to approximate the variables in the function as a power series with the scaling factor α . Following, a reference solution defined as *germ solution*, is calculated for $\alpha = 0$. This way the calculation of the coefficients of the power series in a recursive manner is enabled. Finally, the Padé approximation is used in order to extend the series convergence radius, reaching thus its maximum domain.

3.2 Holomorphic Functions

A holomorphic function is a complex-valued analytic function of one or more complex variables that is, at every point of its domain, infinitely complex differentiable in a neighborhood of the point. The existence of this complex derivative in its neighborhood is a very strong condition since it implies that, any holomorphic function is infinitely differentiable and, more importantly, locally equal to its own Taylor series [12]. This is the main property exploited in this new method for solving nonlinear complex systems.

Since the holomorphic functions are infinitely complex differentiable and complex differentiation is linear, thus obeys the product, quotient and chain rules. The sums, products and compositions of holomorphic functions are also holomorphic, and the quotient of two holomorphic functions is also holomorphic as long as the denominator is not zero.

The use of holomorphic functions as the systems variables is what enables this recursive approach for solving nonlinear systems. Since holomorphic functions have the property of being expanded into a power series such as the Maclaurin series the opportunity of calculating the series coefficients degree by degree allows a recursive manner to solve the system.

3.3 Power Series Expansion of Holomorphic Functions

The Maclaurin series of a generic function $f(\alpha)$ is generated when a Taylor series is expanded about zero:

$$f(\alpha) = \sum_{i=0}^{\infty} c[i]\alpha^i = \sum_{i=0}^{\infty} \frac{f^{(i)}(\alpha)}{i!}, \text{ for } |\alpha| \leq r \quad (3.1)$$

where α is the holomorphic embedding parameter, $f^{(i)}(\alpha)$ is the i -th derivative of $f(\alpha)$ and r is a convergence radius.

Assuming that any electrical variable of a problem can be modeled as a holomorphic function with the right choice of parameters, as for instance the power output generated by one of the systems generators, P_{ij} , can be expanded and approximated for n terms as a power series [9]

$$P_{ij}(\alpha) = \sum_{k=0}^n P_{ij}[k]\alpha^k, \text{ for } |\alpha| < r \quad (3.2)$$

Once the desired system variable becomes a holomorphic function that can be expanded into its Maclaurin's series, the next step is to embed the function with the complex parameter, α . This process will enable the calculation of *germ solution* via a linear system and subsequently, the recursive calculation of the rest of the power series parameters.

3.4 Holomorphic Embedding of Nonlinear Equations

The first step towards using the HEM is to transform the nonlinear system with all kinds of variables into a nonlinear system with variables that are holomorphic embedded functions. The function embedding can be done in several ways, since there is no fixed strategy for it. The general rule for the holomorphic embed is presented in the following steps, where $x(\alpha)$ passes as the system variable that will become the holomorphic embedded function. Note that at this point all the variables are considered already holomorphic functions. To perform the embedding, the following steps are used as example:

- Separate all the nonlinear terms of the equation to the left-hand side of the equation, leaving the rest of the linear and fixed terms on the right-hand side (3.3);

$$-rx^2 = sx + t, x(\alpha) = \sum_{i=0}^n x[i]\alpha^i, \text{ for } |\alpha| < r \quad (3.3)$$

- Insert on the left-hand side of the equation the embedding parameter α (3.4);

$$(-rx^2)\alpha = sx + t \quad (3.4)$$

- Check if the function was successfully embedded by making $\alpha = 0$ (3.5) and getting a linear equation and by making $\alpha = 1$ and getting the original equation (3.6);

$$\alpha = 0, 0 = sx + t \quad (3.5)$$

$$\alpha = 1, -rx^2 = sx + t \quad (3.6)$$

In case the system presents a combination of both linear equations and nonlinear equations there are two ways of guaranteeing the correct embedding;

- First way is to only embed the nonlinear equations resulting in this type of system (3.7);

$$\begin{aligned} (-rx^2)\alpha &= sx + t \\ 0 &= ux + v \end{aligned} \quad (3.7)$$

- Second way is to embed all the equations whether they are linear or nonlinear like shown in (3.8).

$$\begin{aligned} (-rx^2)\alpha &= sx + t \\ -v(1 - \alpha) &= ux \end{aligned} \tag{3.8}$$

Note that this manner of holomorphic embedding, where the linear function is multiplied by the term $(1 - \alpha)$ can also be used for nonlinear equations if all the nonlinear terms are not moved to the left-hand side of the equation.

The difference in the two ways of embedding meshed systems will only appear in the B matrix ($AX = B$) when calculating the power series terms for the *germ solution* and first degree, the rest of the degrees will be the same for either way of embedding the system. The resulting linear systems for calculating recursively the Maclaurin's coefficients can be seen in the equations (3.9) to (3.12) that evidence the subsequent equations systems for $n = 0, 1, 2, 3$. Although it was only represented the systems for all equations embedded with the scaling factor, the presence of not embedded equations does not imply that there are variables that are not holomorphic functions in the system, all of the systems variables will be holomorphic whether or not the linear equations are multiplied by the scaling factor α .

$$\begin{aligned} s_1x_1 &= -t_1 \\ n = 0 \quad s_2x_2 &= -t_2 \\ s_3x_3 &= -t_3 \end{aligned} \tag{3.9}$$

$$\begin{aligned} s_1x_1 &= -r_1x_1^2[0] \\ n = 1 \quad s_2x_2 &= -r_2x_2^2[0] \\ s_3x_3 &= t_3 \end{aligned} \tag{3.10}$$

$$\begin{aligned} s_1x_1 &= -r_1(2x_1[0]x_1[1]) \\ n = 2 \quad s_2x_2 &= -r_2(2x_2[0]x_2[1]) \\ s_3x_3 &= 0 \end{aligned} \tag{3.11}$$

$$\begin{aligned} s_1x_1 &= -r_1(2x_1[2]x_1[0] + x_1^2[1]) \\ n = 3 \quad s_2x_2 &= -r_2(2x_2[2]x_2[0] + x_2^2[1]) \\ s_3x_3 &= 0 \end{aligned} \tag{3.12}$$

Completed the recursive determination of the power series terms you may calculate the problem result by setting the embedded parameter α to unity. However this is not advised since the power series has a very limited radius of convergence thus an extension of the convergence radius is in order, this is achieved by analytic continuation, more specifically by a Padé approximant.

3.5 Analytic Continuation and Padé Approximants

Analytic continuation is a technique to extend the convergence radius of a given power series. The maximal analytic continuation of a power series can be achieved by calculating its diagonal or near-diagonal Padé approximant. The difference between the two are: whether or not the continued fraction is truncated at an even number of terms. The approximant can be written as a rational function of two polynomials which are computed from the finite power series with n terms, in order to obtain an analytical identity as follows [12], [40]:

$$P_i(\alpha) = [L/M]_\alpha = \frac{a[0] + a[1]\alpha + \dots + a[L]\alpha^L}{1 + b[1]\alpha + \dots + b[M]\alpha^M} = \sum_{n=0}^{\infty} P_i[n]\alpha^n \quad (3.13)$$

where L and M are the degree related to the numerator and denominator of the rational function, respectively, and n is the degree of the power series.

A near-diagonal Padé approximant is a rational approximant in which the module of the difference between the polynomial degree of the numerator and denominator is equal to 1, i.e. $(|L - M| = 1)$, whereas in the diagonal Padé approximant the polynomial degree of the numerator and denominator are equal, i.e. $L = M$. Both diagonal or near-diagonal sequence of Padé approximants have been proved to converge to the desired solution [9], [29], but in this work for simplicity we have used only the near-diagonal Padé approximant.

The Padé approximant coefficients, numerator a_i and denominator b_i , can be calculated as linear systems whose equations originate from a discrete convolution. The denominator function convoluted with the Taylor's expansion of $P_i(\alpha)$ is equal to the numerator's function (3.14). From this relation it is possible to separate each of the powers series degrees into one equation of the linear system (3.15).

$$a[0] + a[1]\alpha + \dots + a[L]\alpha^L = (1 + b[1]\alpha + \dots + b[M]\alpha^M) * \left(\sum_{n=0}^{\infty} P_i[n]\alpha^n \right) \quad (3.14)$$

$$\begin{aligned} a[0] &= P_i[0] \\ a[1] &= b[1]P_i[0] + P_i[1] \\ a[2] &= b[2]P_i[0] + b[1]P_i[1] + P_i[2] \\ a[3] &= b[3]P_i[0] + b[2]P_i[1] + b[1]P_i[2] + P_i[3] \\ &\vdots \\ &\vdots \\ &\vdots \end{aligned} \quad (3.15)$$

Rearranging the system presented in (3.15) for a near-diagonal Padé approximant in a matrix form yields in (3.16)

$$\begin{bmatrix} 1 & 0 & 0 & 0 \\ 0 & 1 & -P_i[0] & 0 \\ \vdots & \vdots & \vdots & \vdots \\ 0 & 0 & -P_i[1] & -P_i[0] \\ 0 & 0 & -P_i[2] & -P_i[1] \\ \vdots & \vdots & \vdots & \vdots \end{bmatrix} \begin{bmatrix} a[0] \\ a[1] \\ \vdots \\ b[1] \\ b[2] \\ \vdots \end{bmatrix} = \begin{bmatrix} P_i[0] \\ P_i[1] \\ \vdots \\ P_i[2] \\ P_i[3] \\ \vdots \end{bmatrix} \quad (3.16)$$

Therefore the basic problem consists in firstly transforme all the variables into holomorphic embedded functions and compute the coefficients $P_i[n]$ of the power series. Secondly, from the power series it is needed to determine the coefficients $a[i], i = 0, 1, 2, \dots, L$ and $b[j], j = 1, 2, \dots, M$ of the polynomial rational fraction. Finally, the desired value $P_i(1)$ is computed, i.e., when $\alpha = 1$ the result for the variable of interest will be determined [9].

3.6 Matrix Representation of the Taylor Series Coefficients for a General System

A basic system with three equations (two nonlinear and one linear) can be adapted in two different ways. The first manner all equations are embedded with the complex parameter α , the other only the nonlinear equations are embedded. Bellow the two systems are represented in the matrix model ($AX = B$).

Using the first method, the representation of the matrices are:

$$n = 0 \begin{bmatrix} s_1 & 0 & 0 \\ 0 & s_2 & 0 \\ 0 & 0 & s_3 \end{bmatrix} \begin{bmatrix} x_1[0] \\ x_2[0] \\ x_3[0] \end{bmatrix} = \begin{bmatrix} -t_1 \\ -t_2 \\ -t_3 \end{bmatrix} \quad (3.17)$$

$$n = 1 \begin{bmatrix} s_1 & 0 & 0 \\ 0 & s_2 & 0 \\ 0 & 0 & s_3 \end{bmatrix} \begin{bmatrix} x_1[1] \\ x_2[1] \\ x_3[1] \end{bmatrix} = \begin{bmatrix} -r_1 x_1^2[0] \\ -r_2 x_2^2[0] \\ t_3 \end{bmatrix} \quad (3.18)$$

$$n = 2 \begin{bmatrix} s_1 & 0 & 0 \\ 0 & s_2 & 0 \\ 0 & 0 & s_3 \end{bmatrix} \begin{bmatrix} x_1[2] \\ x_2[2] \\ x_3[2] \end{bmatrix} = \begin{bmatrix} -r_1(2x_1[0]x_1[1]) \\ -r_2(2x_2[0]x_2[1]) \\ 0 \end{bmatrix} \quad (3.19)$$

$$n = 3 \begin{bmatrix} s_1 & 0 & 0 \\ 0 & s_2 & 0 \\ 0 & 0 & s_3 \end{bmatrix} \begin{bmatrix} x_1[3] \\ x_2[3] \\ x_3[3] \end{bmatrix} = \begin{bmatrix} -r_1(2x_1[2]x_1[0] + x_1^2[1]) \\ -r_2(2x_2[2]x_2[0] + x_2^2[1]) \\ 0 \end{bmatrix} \quad (3.20)$$

It is possible to notice that the A matrix does not change as the coefficients for each degree are calculated only matrix B must be updated. It is also possible to notice that terms that were previously nonlinear, matrix B , are now calculated via a Newton binomial formula using the coefficients of the Taylor series.

Using the second method the representation of the matrices are:

$$n = 0 \begin{bmatrix} s_1 & 0 & 0 \\ 0 & s_2 & 0 \\ 0 & 0 & s_3 \end{bmatrix} \begin{bmatrix} x_1[0] \\ x_2[0] \\ x_3[0] \end{bmatrix} = \begin{bmatrix} -t_1 \\ -t_2 \\ -t_3 \end{bmatrix} \quad (3.21)$$

$$n = 1 \begin{bmatrix} s_1 & 0 & 0 \\ 0 & s_2 & 0 \\ 0 & 0 & s_3 \end{bmatrix} \begin{bmatrix} x_1[1] \\ x_2[1] \\ x_3[1] \end{bmatrix} = \begin{bmatrix} -r_1 x_1^2[0] \\ -r_2 x_2^2[0] \\ 0 \end{bmatrix} \quad (3.22)$$

$$n = 2 \begin{bmatrix} s_1 & 0 & 0 \\ 0 & s_2 & 0 \\ 0 & 0 & s_3 \end{bmatrix} \begin{bmatrix} x_1[2] \\ x_2[2] \\ x_3[2] \end{bmatrix} = \begin{bmatrix} -r_1(2x_1[0]x_1[1]) \\ -r_2(2x_2[0]x_2[1]) \\ 0 \end{bmatrix} \quad (3.23)$$

$$n = 3 \begin{bmatrix} s_1 & 0 & 0 \\ 0 & s_2 & 0 \\ 0 & 0 & s_3 \end{bmatrix} \begin{bmatrix} x_1[3] \\ x_2[3] \\ x_3[3] \end{bmatrix} = \begin{bmatrix} -r_1(2x_1[2]x_1[0] + x_1^2[1]) \\ -r_2(2x_2[2]x_2[0] + x_2^2[1]) \\ 0 \end{bmatrix} \quad (3.24)$$

The only difference between the two forms of holomorphic adaptation are in the matrix B for $n=0,1$ in the lines equivalent to the linear equations.

3.7 Overview of The Holomorphic Embedding Load Flow Method

A flowchart about the Holomorphic Embedding Method is shown in the Fig. 3.1

3.8 State of the Art about Some Existing Holomorphic Embedding Method Approaches

As of the moment there are only a few works that apply the holomorphic embedding method, some of the most significant are:

- The Holomorphic Embedding Load Flow method [9]: The pioneer work applying HEM in an electrical problem. This paper applies this technique of holomorphic embedding into the load flow problem.
- Efficient Holomorphic Based Approach for Unit Commitment Problem [13]: Uses HEM as a tool for solving the the power flow problem within the Unit Commitment (UC) problem. The later is solved by Particle Search Space (PSS) algorithm.
- Multi-Stage Holomorphic Embedding Method for Calculating the Power-Voltage Curve [48]: Uses a multi-stage HEM approach in order to reduce the error and increase the convergence speed close to the nose point of the PV curve.

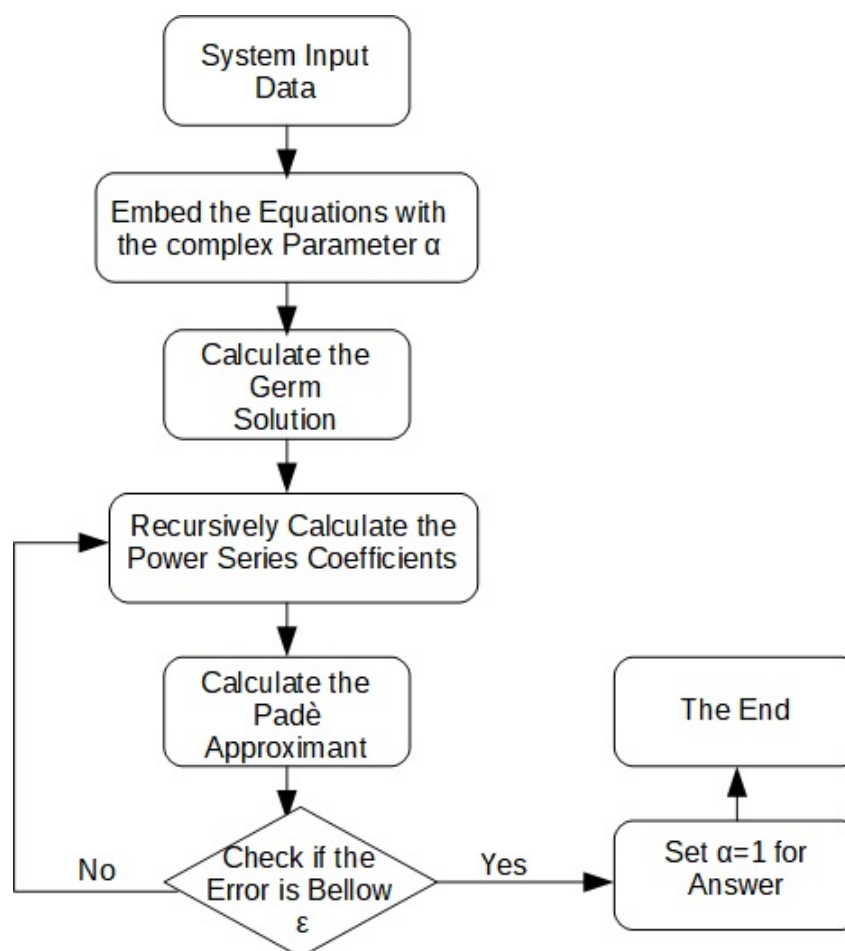


Figure 3.1: Traditional HEM Flowchart

- A Holomorphic Embedding Method to Solve Unstable Equilibrium Points of Power Systems [47]: Uses the Holomorphic method to solve an equivalent Power Flow problem considering generators speeds to find the unstable equilibrium point of the system.
- Voltage Stability Analysis of Power Systems With Induction Motors Based on the Holomorphic Embedding [14]: Applies a set of methods based on HEM to solve steady state and dynamic state of a power system with induction motors.
- Nonlinear network reduction for distribution networks using the holomorphic embedding method [10]: Uses the HEM to solve the power flow problem within the network reduction. The PF acts as a base line for the system reduction.

3.9 Conclusion of this Chapter

In this chapter was introduced the concept of holomorphic functions and its properties, the process to embed with a complex parameter holomorphic functions. It was also presented the analytic continuation, the Padé approximant, the general formula for the HEM and its characteristics equations.

There were also some brief descriptions of the most relevant works done with the holomorphic embedding approach for solving different types of problems, such as the power flow problem [9], the unit commitment problem [7, 13], the network reduction problem [10], equilibrium points solution [47], the power voltage curve calculation [48] and the voltage stability [14] problem all which are nonlinear.

Chapter 4 THE HOLOMORPHIC EMBEDDING METHOD USED FOR SOLVING THE ECONOMIC DISPATCH PROBLEM

4.1 Introduction

In this chapter, the Holomorphic Embedding Method is applied to the Economic Dispatch Problem. The problem formulation is detailed for a generic case. It is presented the problem model, the holomorphic embedding strategy, the equations and associated matrices, the methodology and the schematic for implementation.

To the full knowledge of the authors, the method has never been used before for solving this type of problem. A recent work was proposed for solving the Unit Commitment Problem (UCP) [13]. However, on that case the method was used not for the nonlinear system solution but for the load-flow solution as part of the UCP algorithm.

In this dissertation, the equations of the nonlinear system are all transformed into holomorphic functions and then solved in a recursive manner using a Taylor series followed by a Padé approximation. This process enables a more accurate solution and less dependent on the initial guess.

4.2 Problem Formulation

The Economic Dispatch Problem consists in supplying a given electrical power at the minimum cost possible abiding to the problem's nature restrictions such as the Kirchhoff's Laws and the machine's operational limits.

There are many possible restrictions due to the electrical nature of the problem that are possible to be investigated. In this dissertation, there are considered the following ones:

- Power balance at each bus;
- Machine's upper and lower operational limits.

The first restriction is a equality constraint which is present at any moment, regardless of the power output of a given generating unit. The power balance equation at a bus i , where is connected a lumped load, L_i and a power generation with N_{gi} thermal units generating P_{ij} , is :

$$\sum_{i=1}^{N_{gi}} P_{ij} = L_i + \sum_{m \in \Omega_i} P_{Dim} \quad (4.1)$$

where Ω_i is a set of buses which has connection with the bus i ; P_{Dim} is the active power flowing from the bus i to bus m .

The power flowing from i to m is approximated by the quadratic function:

$$P_{Dim} = -b_{im}\theta_{im} + \frac{g_{im}\theta_{im}^2}{2}, \quad i = 1, \dots, N_b, m \neq i \quad (4.2)$$

where $\theta_{im} = \theta_i - \theta_m$ and $y_{im} = g_{im} + jb_{im}$ is the longitudinal admittance connecting the buses $i - m$.

Therefore, from (4.2) the load flow at the interconnection $i - m$ are $P_{FL}^{im} = P_{Dim} + P_{Dmi} = g_{im}\theta_{im}^2$.

The second restriction creates inequalities constraints that are only active in the case of a limit violation. These inequalities constraints are of the type $\underline{P}_i \leq P_i \leq \bar{P}_i$, where \underline{P}_i and \bar{P}_i are lower and upper limit, respectively. They are transformed into single equalities constraints (4.3) or (4.4) and then, case needed, it is incorporated to the system's modeling equations.

$$\underline{P}_i - P_i < 0 \quad P_i - \bar{P}_i < 0 \quad (4.3)$$

$$P_i - \underline{P}_i = 0 \quad \bar{P}_i - P_i = 0 \quad (4.4)$$

Therefore using these restrictions the Lagrangian function used for modeling a generic problem is

$$\begin{aligned}
LF(P, \lambda, \theta, \pi) = & \sum_{i=1}^{N_g} \sum_{j=1}^{N_{gi}} F_{ij} - \sum_{k=1}^{N_b} \lambda_k \left[\sum_{j=1}^{N_{gk}} P_{kj} - \sum_{m \in \Omega_k} (-b_{km} \theta_{km} + \frac{g_{km} \theta_{km}^2}{2}) - L_k \right] + \\
& + \sum_{i=1}^{N_g} \sum_{j=1}^{N_{gi}} \underline{\pi}_{ij} (-P_{ij} + \underline{P}_{ij}) + \sum_{i=1}^{N_g} \sum_{j=1}^{N_{gi}} \bar{\pi}_{ij} (P_{ij} - \bar{P}_{ij}) \quad (4.5)
\end{aligned}$$

where F_{ij} is the cost function for the generating unit j connected at the bus i ; Ω_k is a set of buses that has connection with the bus k ; P is a vector whose entries are power output of a generation unit, P_{ij} ; λ is the vector of the Lagrange multiplier associated to each bus, whose entries are λ_k ; θ is the vector with the voltage phases, θ_m , except the $\theta_1 = 0$, which is the reference; π is the vector associated to the violation of limits, whose entries are $\underline{\pi}$ or $\bar{\pi}$.

Note that (4.5) includes only operational constraints of the unit output power.

The nonlinear system characteristic of an EDP is derived from the Lagrangian function (4.5). This system can be presented as forming four blocks of equations. The first block is composed of equations obtained by the partial derivatives in relation to the unit generation power output, (P_{ij}) . They form equations for $i = 1, \dots, N_g$ and $j = 1, \dots, N_{gi}$. These equations are all linear with the following type (4.6). However in the event of a limit violation the equation for the violating unit will be (4.7):

$$\frac{\partial LF(P, \lambda, \theta, \pi)}{\partial P_{ij}} = 2c_{ij} h_{1ij} P_{ij} + c_{ij} h_{2ij} - \lambda_i = 0 \quad (4.6)$$

$$\frac{\partial LF(P, \lambda, \theta, \pi)}{\partial P_{ij}} = 2c_{ij} h_{1ij} P_{ij} + c_{ij} h_{2ij} - \lambda_i + \bar{\pi}_{ij} - \underline{\pi}_{ij} = 0 \quad (4.7)$$

where h_{2ij} and h_{1ij} are parameters of the machine's heat curve, $H_{ij} = h_{1ij} P_{ij}^2 + h_{2ij} P_{ij} + h_{3ij}$, and c_{ij} is the fuel cost for machine i , all associated to the unit j connected at the bus i .

The second group is formed by the equations obtained by partially deriving the Lagrangian around the marginal costs λ_k . This yields nonlinear equations as the one represented in (4.8):

$$\frac{\partial LF(P, \lambda, \theta, \pi)}{\partial \lambda_k} = - \sum_{j=1}^{N_{gk}} P_{kj} + \sum_{m \in \Omega_k} [(-b_{km} \theta_{km} + \frac{g_{km} \theta_{km}^2}{2}) + L_k] = 0, \quad k = 1, \dots, N_b \quad (4.8)$$

The third group comprises the equations formed when the Lagrangian function is derived with respect to θ_m . The equations in this group can be represented by the subsequent equation (4.9).

$$\frac{\partial LF(P, \lambda, \theta, \pi)}{\partial \theta_k} = \lambda_k \sum_{m \in \Omega_k} (-b_{km} + g_{km} \theta_{km}) + \sum_{k \in \Omega_m} \lambda_m (b_{mk} - g_{mk} \theta_{mk}) = 0, \quad k = 2, \dots, N_b \quad (4.9)$$

The final group is composed of the equations formed by differentiating the Lagrangian function around $\bar{\pi}_{ij}$ or $\underline{\pi}_{ij}$. This set of equations only exists when there is a limit violation. Nonetheless, they can be in one of two of the following forms, depending on whether it was an upper limit violation (4.10) or a lower limit violation (4.11):

$$\frac{\partial LF(P, \lambda, \theta, \pi)}{\partial \bar{\pi}_{ij}} = P_{ij} - \bar{P}_{ij} = 0 \quad (4.10)$$

$$\frac{\partial LF(P, \lambda, \theta, \pi)}{\partial \underline{\pi}_{ij}} = -P_{ij} + \underline{P}_{ij} = 0 \quad (4.11)$$

In the next section the embedding problem is formulated considering the set of equations (4.6)-(4.11).

4.3 The Holomorphic Embedding Method Strategy

The holomorphic embedding method can be applied in many different forms. For instance, it can be employed only as a tool for solving a load flow and therefore calculating the losses. Or it can be used as in the case of this work for solving the nonlinear characteristic system applied to the EDP. There are inexhaustible manners for the holomorphic embedding of the equations. In this work, we proposed a technique based on the residues of nonlinear equations. To better illustrate the embedding problem, it is presented a tutorial example for a quadratic model in the sequel.

The problem is described as follows. Given a generic nonlinear equation $F(x) = 0$, $x \in \mathbb{R}^n$, $F(x) \in \mathbb{R}^n$ and a guess x_0 of the roots. The first objective is to determine a power series that approximate $F(x)$ to find its root x . In the sense of holomorphic embedding function, the main step consists in approximating the function $F(x)$ and the solution x by a Taylor's series as a function of the scaling factor α .

$$F(x(\alpha)) = F[0] + F[1]\alpha + F[2]\alpha^2 + \dots + F[m]\alpha^m \quad (4.12)$$

$$x(\alpha) = x[0] + x[1]\alpha + x[2]\alpha^2 + \dots + x[m]\alpha^m \quad (4.13)$$

Suppose that the residue (mismatch) of $F(x)$ for the guess $x_0 = x[0]$ is $R = F(x_0) = F[0]$. Therefore, if we embed the equation $F(x) = 0$ by

$$F(x) = (1 - \alpha)R \quad (4.14)$$

the seed solution (degree zero of the power series) leads to $F(x_0) = F[0] = R$. However, the final solution is found numerically when $\alpha = 1$. In fact, when $\alpha = 1$ in (4.14), $F(x(\alpha)) = 0$, indicates that $x(1)$ is the solution of the equation.

Since $x[0] = x_0$, the other coefficients of $x(\alpha)$, for $m = 1, 2, \dots$ are computed substituting the expression (4.13) for $x(\alpha)$ in $F(x(\alpha)) = F(x[0] + x[1]\alpha + x[2]\alpha^2 + \dots)$. Then, in the next step, is needed to identify the coefficients in α for both sides of the equation (4.14), assuming $F(x)$ is expanded as in (4.12). Note that a coefficient $F[k]$ must be explicitly found as a function of the yet to be determined, $x[k]$, and the historic terms $x[0], x[1], \dots, x[k-1]$.

Initiating by the degree $m = 1$ (polynomial with degree 1) in (4.13), the term $x[1]$ can be computed. It is substituted the values for $x(\alpha)$ as $F(x[0] + x[1]\alpha)$. Then, the coefficients of the power α^1 from both sides of the expanded power series are identified. This is a linear system in the variable $x[1]$ and right hand side equal to $-R$.

For $m = 2$ (polynomial with degree 2), the focus is to calculate $x[2]$. Again, as in the case for $m = 1$, we use $x(\alpha)$ to obtain $F(x[0] + x[1]\alpha + x[2]\alpha^2)$. Now, we need to match coefficients for the term α^2 at both sides of the equation in (4.14), $F(x)$ must be in the form of a power series. For $m \geq 2$, the terms at right side of the equation vanish, because the maximum degree on this side is 1. While, at left-hand side, we have the terms as a function of $x[0], x[1]$ and $x[2]$, forming a linear system around the variable $x[2]$. The other coefficients of the power series, $x[k], k = 3, 4, \dots$ can be calculated similarly until a finite order of interest. This latter order is defined according to the objective imposed by the user, such as a given precision for the mismatch $F(x(\alpha))$ or even a given order m_{max} .

The nonlinear EDP equations treated in this dissertation are of the quadratic type. Thus, to illustrate the embedding model previously described, consider the single variable equation $5x^2 - 6x + 1 = 0$. This equation has the exact roots $x = 1$ and $x = 0.2$. Suppose that the search by a root starts with the seed solution (estimate) $x_0 = 2$. Then, this guess generates the mismatch $R = F(x_0) = 9$. Considering

$$x(\alpha) = x[0] + x[1]\alpha + x[2]\alpha^2 + \dots,$$

the embedding model is

$$5 [x[0] + x[1]\alpha + x[2]\alpha^2 + \dots]^2 - 6 [x[0] + x[1]\alpha + x[2]\alpha^2 + \dots] + 1 = (1 - \alpha) \cdot 9 \quad (4.15)$$

Clearly the value $x[0] = x_0 = 2$ satisfies the degree zero in (4.15), since $5x[0]^2 - 6x[0] + 1 = 9$. Identifying the coefficients of α^1 for both sides in (4.15), following equation for the unknown $x[1]$ is obtained: $10x[0]x[1] - 6x[1] = -9$. The solution for it is $x[1] = -9/14$. Now, for computing $x[2]$, the quadratic term equation (4.15) is expanded until degree 2 and then set it to zero, since the maximum degree in α at the right hand side of the equation (4.15) is 1. This result yields in $10x[0]x[2] + 5x[1]x[1] - 6x[2] = 0$. Therefore, $10x[0]x[2] - 6x[2] = -5x[1]x[1]$, whose solution is $x[2] = -405/2744$. For degree 3, the following equation is obtained: $10x[0]x[3] + 10x[1]x[2] - 6x[3] = 0$, or $10x[0]x[3] - 6x[3] = -10x[1]x[2]$, yielding in $x[3] = -36450/537824$. Computing the term $x[4]$, the value $x[4] = -0.0342$ is found. The approximated value for $x(\alpha)$ by considering $\alpha = 1$ and the the sum of the coefficients of the power series up to the 4th degree is equal to 1.1075.

In order to circumvent the small convergence radius originated by approximating x through the sum of the power series terms for $\alpha = 1$, the polynomial is approximated by a rational fraction called the Padé approximant. This approximation is made for the example in question, considering the 4th degree power series.

Assume that the rational fraction which need to be identified from the power series is of the type:

$$x(\alpha) = \frac{a_0 + a_1\alpha + a_2\alpha^2}{1 + b_1\alpha + b_2\alpha^2} = x[0] + x[1]\alpha + x[2]\alpha^2 + x[3]\alpha^3 + x[4]\alpha^4.$$

The identification of the rational fraction is then carried out to satisfy the identity:

$$a_0 + a_1\alpha + a_2\alpha^2 = [1 + b_1\alpha + b_2\alpha^2][x[0] + x[1]\alpha + x[2]\alpha^2 + x[3]\alpha^3 + x[4]\alpha^4]$$

This means that $a_0 = x[0]$, $a_1 = b_1x[0] + x[1]$, $a_2 = b_2x[0] + b_1x[1] + x[2]$. Also, $0 = b_2x[1] + b_1x[2] + x[3]$ and $0 = b_2x[2] + b_1x[3] + x[4]$. From these two last equations, the coefficients b_1 and b_2 are computed, yielding $b_1 = -0.5510$ and $b_2 = 0.0211$. This implies that $a_0 = x[0] = 2$, $a_1 = -1.7449$ and $a_2 = 0.2448$. Then the approximation for the Padé approximant model assuming $\alpha = 1$ yields $x = 1.072$.

Both the results computed by the Padé approximation and the one calculated based on the Taylor's series coefficient sum indicate possible convergence to the root $x = 1$. The convergence result reached by the Padé approach is better than the convergence for the sum of the series coefficients. However, the best result $x = 1.072$ gives a mismatch equal to 0.3139. Obviously, this result is far away from a desired result, which assure a high accuracy for the solution. To control the precision of the solution, and the mismatch accuracy was defined as 10^{-8} . The result concerning the value x could be improved by augmenting the number of coefficients of the power series. However, it might require a very high degree for the power series. Also, the process of dealing with elevated order power series generates coefficients with very low (or high) values. This fact leads to a numerical truncation problem and causes the approximated numerical value of x to stagnate far from the effective solution, even with the increase on the order of the power series.

Then, to improve the quality of the solution and considering a very low order for the power series, we adopt the technique proposed in [11]. By the technique proposed in that work, a low order degree power series is calculated and so the Padé approximant. The key aspect considered is the adoption of a restart process, in which the procedure of calculating the coefficients of the series is recalculated. That is, the calculation process is re-initiated, but now with a new, more solution-oriented seed (guess), based on the last solution obtained by Padé approximation for $\alpha = 1$. Then, giving procedure to the previous example, it is proposed to restart the process there. Hence, the power series coefficients computation is restarted with the estimate $x_0 = 1.072$ (seed $x[0] = 1.072$).

Considering the restart with the new value for x_0 , a mismatch $F(x_0) = 0.3139$ is initially found. Next, the residue R is assigned as $R = F(x_0) = 0.3139$. Following

the same procedure applied for the calculus performed previously, new power series coefficients are computed, as well as new Padé approximant. The coefficients found for the power series are: $x[0] = 1.072$, $x[1] = -0.0665$, $x[2] = -0.00468$, $x[3] = -6.6 \times 10^{-4}$ and $x[4] = -1.023 \times 10^{-4}$. The coefficients for the polynomials of the Padé rational fraction are: $b_1 = -0.1691$, $b_2 = 0.0020$, $a_0 = 1.0720$, $a_1 = -0.2477$ and $a_2 = 0.0087$. The approximated values for x when $\alpha = 1$, computing via Padé approximant and sum of power series coefficients are 1.000024 and 1.000043, respectively. The mismatch computed for the Padé approximant solution yields 9.6×10^{-5} . Since this result does not satisfy a mismatch tolerance 10^{-8} , a *second restart* is need. Therefore, restarting the process by starting with $x_0 = 1.000024$, the solution $x = 1.0$ is found with mismatch zero for both the Padé approximant and sum of the power series coefficients values.

To compare the performance of the holomorphic embedded method, the same example was solved by using the classical Newton-Raphson method. The same initial estimate $x_0 = 2$ has been adopted. The NR method took six iterations to find the solution $x = 1$ and reach a mismatch smaller than 10^{-8} .

An interesting result verified for the computations of the coefficients for $m \geq 1$ is that the term $10x[0]x[m] - 6x[m]$ appears in all computations, where the unknown is $x[m]$. This is exactly the result for the first derivative of the function $F(x)$ at an iteration $x = x_k$, $k = 0, 1, 2, \dots$ when the NR is used. This result is also verified for multivariate systems. In this situation the first derivative is the Jacobian matrix of the Newton-Raphson method. Another remark is that for computing the power series coefficients, the right hand side of the resulting linear system is formed from historic values $x[1], x[2], \dots, x[m-1]$. Hence, along the computation of the coefficients the Jacobian matrix stays constant.

In the next section, the holomorphic embedding model discussed beforehand will be extended to EDP. The idea is to keep the same embedding model based on the residues of the nonlinear equations.

4.4 The Holomorphic Embedding Model for the EDP

In this section, the HEM is applied to EDP. The technique based on the residue embedding technique is imposed to the problem. The objective is to solve the set of equations (4.6)-(4.10). With this aim, consider that this set of equations can be put

as $F(x) = 0$, where $F(x) \in \mathbb{R}^n$ and $x \in \mathbb{R}^n$ is the vector $x^T = [P^T \ \lambda^T \ \theta^T \ \pi^T]$, with $n = 3N_g N_{gi} + (2N_b - 1)$. For this value of n , $2N_g N_{gi}$ of the variables are regarding the slack-variables π . On this work, they are activated just when an operational limit of a generation unit is violated and always, only one side of the limit is violated. Therefore, we should have in mind that only a very limited number of variables are violated, leading to a very reduced number of nonzero slack-variables. In case of no violation, n can be treated as $n = N_g N_{gi} + (2N_b - 1)$.

As discussed in the Section 4.3, the first step to holomorphically embed the equations consists in defining a seed solution or estimate x_0 . After this procedure, the seed solution is set to $x[0] = x_0$ and the residue $R = F(x_0)$ is computed.

An obvious challenge is to establish the seed solution. This is a task that must be achieved by a much easier strategy than the calculation of the final solution of the nonlinear problem. In the load flow problem originally presented by Trias [9], and presented for a multibus system in [12], the seed solution was proposed as the slack-bus voltage replicated for all system buses. This consideration is quite satisfactory from a physical point of view, since the voltages on the physical buses are close to the nominal voltage. Similarly, for the case of the EDP, we propose to set the solution of the lossless EDP as the seed solution. This fact is justified, because the losses in the system are due to ohmic losses at the transmission lines and they have very reduced values, when compared to the bulk of transmitted power. In this sense, it is expected the seed solution this way assigned be an adequate estimate for the HEM applied to EDP, considering restart.

The lossless EDP solution can be determined through the solution of the equation set (4.6)-(4.10), by setting $g_{km} = 0$ for all interconnection $k - m$. Proceeding this way, a linear system must be solved for the variable x as defined previously. This result is used as the seed solution $x[0]$ or estimate x_0 for the Restarted Holomorphic Embedding Method discussed in the Section 4.3.

The seed solution is then used for the calculation of the residues (mismatches), R_ℓ , $\ell = 1, \dots, (3N_g \cdot N_{gi} + 2N_b - 1)$, for the the set of equations (4.6)-(4.10). The residue R will be also used as an element to evaluate the accuracy of convergence in the computation of the process solution.

In the sequence, the Taylor's series for each variable is determined. Afterwards,

a Padé approximant is calculated. The process is restarted using the latter solution obtained from the Padé approximant [11], instead of the lossless EDP solution. Since it is adopted a restarted approach, the final result will be obtained from the last Padé approximant, when a tolerance for the mismatch is reached. The flowchart in Fig. 4.1 illustrates a simplified procedure on the main steps of the computational process.

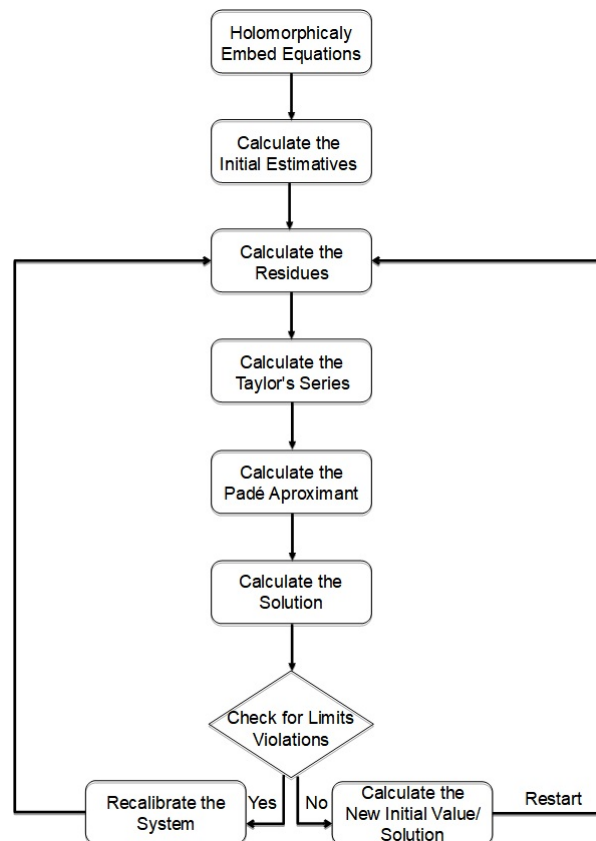


Figure 4.1: Restarted HEM Flowchart

The EDP is conceived using all generation connected to a bus $i = 1, 2, \dots, N_b$ and an equivalent load L_i bulked at the same bus i . A bus can have only generation, or only load or both components. This configuration yields a single value of λ for all buses k , λ_k . All initial estimate for θ_m are obtained from the θ_m calculated from the lossless EDP. Also, the bus 1 is assumed as the angular reference with $\theta_1 = 0$. All estimates for the initial power, P_{ij} , are also defined from the lossless problem solution.

4.4.1 Embedding Equations Based on the Residue

Once the residue $R = F(x_0) \in \mathbb{R}^n$ is computed, the equations are embedded as follows. The first block of equations yields:

$$2c_{ij}h_{1ij}P_{ij} + c_{ij}h_{2ij} - \lambda_i = R_\ell[1 - \alpha], \quad \ell = 1, \dots, N_g \cdot N_{gi}, \quad i = 1, \dots, N_g, \quad j = 1, \dots, N_{gi} \quad (4.16)$$

For equation (4.16), in the case of a violation of any limit, the violated power P_{ij} must be fixed in the value \underline{P}_{ij} or \overline{P}_{ij} . Together with the rest of the equation the respective slack-variable ($-\underline{\pi}_{ij}$ or $+\overline{\pi}_{ij}$) is needed to be added to the left-hand side of the equation, according to (4.8).

The second block of equations are related to the derivatives with relation to λ_k . The expressions are embedded as

$$\sum_{j=1}^{N_{gk}} P_{kj} - \sum_{m \in \Omega_k} (-b_{km}\theta_{km} + \frac{g_{km}\theta_{km}^2}{2}) - L_k = R_k[1 - \alpha], \quad k = 1, \dots, N_b \quad (4.17)$$

The third block of equations is associated with the derivatives with respect to θ_m . The nonlinear equations are embedded of the following form:

$$\lambda_k \sum_{m \in \Omega_k} (-b_{km} + g_{km}\theta_{km}) + \sum_{k \in \Omega_m} \lambda_m (b_{mk} - g_{mk}\theta_{mk}) = R_k[1 - \alpha], \quad k = 2, \dots, N_b \quad (4.18)$$

The fourth block of equations is associated to the slack-variables π . No action is need to impose to this type of variable with relation to the embedding process, because it is inserted in (4.16) exactly as a slack-variable and the violated power is fixed at its respective limit value. i.e., the power is no more unknown.

The system variables comprising (4.16)-(4.18) are now a function of the scaling factor α , i.e., $P_{ij}(\alpha)$, $\lambda_k(\alpha)$ and $\theta_m(\alpha)$. When P_{ij} has its limit violated, the variable assumes a known value that is equal to its violated limit. This process gives place to a respective slack-variable, which is kept constant, i.e. independent of α , when the solution is searched.

The embedded variables are approximated by truncated Taylor series as (4.19)-(4.21). The initial coefficients for the variables ($P_{ij}[0]$, $\lambda_k[0]$, $\theta_m[0]$) are the same as the ones obtained from the lossless problem solution. Here the generic notation $x[\cdot]$ stands for a Taylor's scalar coefficient.

The further coefficients are calculated in a recursive manner, as a function of historic values. It is important to notice at this point that the Taylor series coefficients must be calculated up to an even degree defined by the user. At the end, a proper fraction Padé approximant must be computed.

$$P_{ij}(\alpha) = P_{ij}[0] + P_{ij}[1]\alpha + P_{ij}[2]\alpha^2 + P_{ij}[3]\alpha^3 + \dots \quad (4.19)$$

$$\lambda_k(\alpha) = \lambda_k[0] + \lambda_k[1]\alpha + \lambda_k[2]\alpha^2 + \lambda_k[3]\alpha^3 + \dots \quad (4.20)$$

$$\theta_m = \theta_m[0] + \theta_m[1]\alpha + \theta_m[2]\alpha^2 + \theta_m[3]\alpha^3 + \dots \quad (4.21)$$

Each coefficient is calculated by a linear equation system formed according to the degree n . The coefficients for the case $n = 0$ are known as the *germ or seed solution*, which we are assumed to be obtained from the lossless EDP solution. Therefore, the coefficients are calculated for the remaining values of n .

For $n = 1$, we need to match terms with degree 1 for α in both sides of (4.16)-(4.18), assuming that all residues R_i were calculated. Then, the following equations of a linear system are determined:

$$2c_{ij}H_{1ij}P_{ij}[1] - \lambda_i[1] = -R_\ell, \quad \ell = 1, \dots, N_g N_{gi}, \quad i = 1, \dots, N_g, \quad j = 1, \dots, N_{gi} \quad (4.22)$$

$$\sum_{j=1}^{N_{gk}} P_{kj}[1] - \sum_{m \in \Omega_k} (-b_{km}\theta_{km}[1] + g_{km}\theta_{km}[1]\theta_{km}[0]) = -R_k, \quad k = 1, \dots, N_b \quad (4.23)$$

$$\begin{aligned} & \lambda_k[1] \sum_{m \in \Omega_k} (-b_{km} + g_{km}\theta_{km}[0]) + \lambda_k[0] \sum_{m \in \Omega_k} (g_{km}\theta_{km}[1]) + \\ & + \sum_{k \in \Omega_m} \lambda_m[1](b_{mk} - g_{mk}\theta_{mk}[0]) - \sum_{k \in \Omega_m} \lambda_m[0]g_{mk}\theta_{mk}[1] = \\ & = -R_k, \quad k = 2, \dots, N_b \end{aligned} \quad (4.24)$$

For the linear equations (4.22)-(4.24) the unknowns are $P_{ij}[1]$, $\lambda_k[1]$ and $\theta_m[1]$. note that $\theta_{km} = \theta_k - \theta_m$, must be separated in θ_k and θ_m in order to solve the linear system.

For $n = 2$, the nonzero term corresponding to the residue for germ solution vanishes, since the coefficients of terms whose degrees are greater than 1 in the right-hand side of (4.16)-(4.18) are all zero. The equations for $n = 2$ are:

$$2c_{ij}h_{1ij}P_{ij}[2] - \lambda_i[2] = 0, \quad i = 1, \dots, N_g, \quad j = 1, \dots, N_{gi} \quad (4.25)$$

$$\sum_{j=1}^{N_{gk}} P_{kj}[2] - \sum_{m \in \Omega_k} (-b_{km}\theta_{km}[2] + g_{km}\theta_{km}[2]\theta_{km}[0]) + \gamma_k = 0, \quad k = 1, \dots, N_b \quad (4.26)$$

$$\begin{aligned} & \lambda_k[2] \sum_{m \in \Omega_k} (-b_{km} + g_{km}\theta_{km}[0]) + \lambda_k[0] \sum_{m \in \Omega_k} (g_{km}\theta_{km}[2]) + \\ & + \sum_{k \in \Omega_m} \lambda_m[2](b_{mk} - g_{mk}\theta_{mk}[0]) - \sum_{k \in \Omega_m} \lambda_m[0]g_{mk}\theta_{mk}[2] + \\ & + \rho_k = 0, \quad k = 2, \dots, N_b \end{aligned} \quad (4.27)$$

where

$$\begin{aligned} \gamma_k &= - \sum_{m \in \Omega_k} \frac{g_{km}}{2} \theta_{km}[1]^2 \\ \rho_k &= \lambda_k[1] \sum_{m \in \Omega_k} g_{km}\theta_{km}[1] - \sum_{k \in \Omega_m} \lambda_m[1]g_{mk}\theta_{mk}[1] \end{aligned}$$

Therefore, the extension of the computation of the coefficients for $n > 2$ consists basically in computing γ and ρ_k . Besides, the linear system involved in the coefficient calculation process requires only the LU factorization for computing the coefficients for $n = 1$.

The coefficients calculated for the Taylor series are then used for obtaining the Padé expansion. This second approximation is used for expanding the convergence radius of the solution [9]. In this work, a diagonal Padé is used, which means that

the numerator and denominator have the same polynomial degree (see (4.28)-(4.30)). Once calculated the Padé rational fraction, the solution is obtained by set the scaling factor α to unit.

$$\begin{aligned} P_{ij} &= P_{ij}[0] + P_{ij}[1]\alpha + P_{ij}[2]\alpha^2 + \dots = \\ &= \frac{a_{P_{ij}}[0] + a_{P_{ij}}[1]\alpha + a_{P_{ij}}[2]\alpha^2 + \dots}{1 + b_{P_{ij}}[1]\alpha + b_{P_{ij}}[2]\alpha^2 + \dots} \end{aligned} \quad (4.28)$$

$$\begin{aligned} \lambda_k &= \lambda_k[0] + \lambda_k[1]\alpha + \lambda_k[2]\alpha^2 + \dots = \\ &= \frac{a_{\lambda_i}[0] + a_{\lambda_i}[1]\alpha + a_{\lambda_i}[2]\alpha^2 + \dots}{1 + b_{\lambda_i}[1]\alpha + b_{\lambda_i}[2]\alpha^2 + \dots} \end{aligned} \quad (4.29)$$

$$\begin{aligned} \theta_m &= \theta_m[0] + \theta_m[1]\alpha + \theta_m[2]\alpha^2 + \dots = \\ &= \frac{a_{\theta_m}[0] + a_{\theta_m}[1]\alpha + a_{\theta_m}[2]\alpha^2 + \dots}{1 + b_{\theta_m}[1]\alpha + b_{\theta_m}[2]\alpha^2 + \dots} \end{aligned} \quad (4.30)$$

In (4.28)-(4.30), the parameters $a_{P_{ij}}$, $b_{P_{ij}}$, a_{λ_k} , b_{λ_k} , a_{θ_m} and b_{θ_m} must be determined accordingly to the Padé identification technique [9].

For a better accuracy and a smaller order for the Taylor series and Padé aproximant, a restarted approach is adopted [11]. Therefore, once the first solution is obtained the results are used as the new guess for HEM. Thus, the residues R_i are updated followed by the calculation of new coefficients and a new rational fraction. Once the accuracy is within the desired value, the final Padé approximant is the EDP partial solution.

Finally, we need to verify whether all operational limits were met. In case of fail, the HEM EDP is solved again considering the violated limits and associated slack-variable. Also, in case of negative value for a slack-variable, this means that the respective limit associated to the slack-variable must be relaxed. The process must go on until all variables meet the operational limits.

4.5 Conclusion of this Chapter

In this chapter, the fundamentals for the constrained holomorphic embedding EDP was presented. Firstly, the general constrained EDP was formulated considering a lossy multibus system. The losses are due to the ohmic effect in transmission losses in the system. They are approximated by a quadratic function, which depends on the conductance of the line and the voltage phase difference between the two line terminals.

The multibus EDP was formulated as an optimization problem, where the objective function is based on the cost of power generation of thermal units, subject to operational limits.

A detailed example was presented with the purpose of illustrating the HEM approach applied to the EDP. Also, a detailed explanation was presented in order to show the strategy to embed the equations of the EDP and solve them, including the handling of operational limits.

In the next chapter, we perform experiments in some test system in order to demonstrate the performance of the technique described in this chapter.

Chapter 5 METHODOLOGY AND RESULTS

5.1 Introduction

In this chapter experiments are carried out with the purpose to demonstrate the efficacy of the holomorphic embedding method applied to the multibus economic dispatch problem. The experiments are assessed in three test systems. The test systems consist of 3-, 9- and 14-bus power system models. The 3-bus model is used to illustrate primal understanding of the proposed method, while the 9- and 14-bus model are IEEE benchmark test systems which were adapted in this work in order to perform simulations characterized by multi-generator connected at a bus. From this three study cases different loading and operating limits scenarios are studied. All systems and scenarios have their results compared to the traditional Newton-Raphson solution method. The error for each method is also evaluated.

All computations were performed in MATLAB.

The results are then compared with each other and analysis regarding the method trustworthiness and significant contributions are made. It is also presented some interpretations of the results and comparative analysis among scenarios.

5.2 Test System Models

In this dissertation, different systems and network topologies are considered. The characterization of each one of the three power system networks is discussed in the sequel.

- System 1: composed of three buses and five generating units as illustrated by the schematic in Fig.5.1;
- System 2: composed of nine buses and eight generating units (see Fig.5.2);

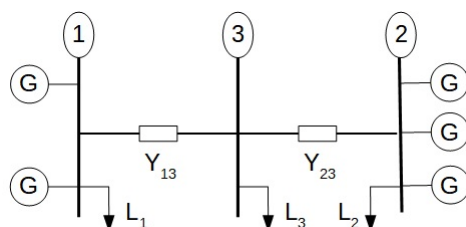


Figure 5.1: 3-bus test system schematic

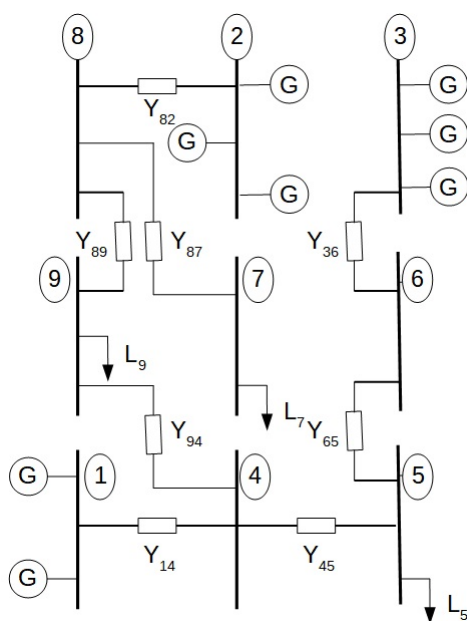


Figure 5.2: 9-bus test system schematic

- System 3: composed of fourteen buses and thirteen generating units (see Fig.5.3);

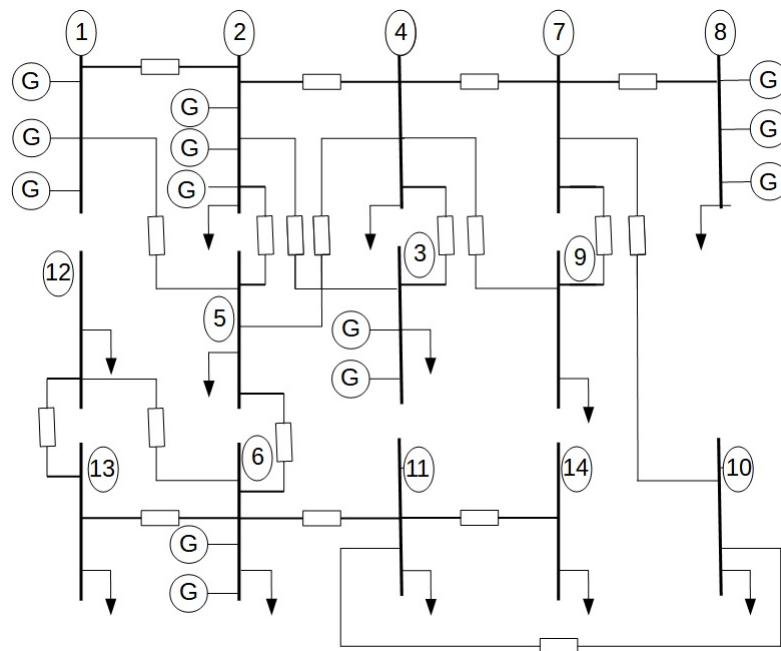


Figure 5.3: 14-bus test system schematic

Each system topology was tested for three different scenarios with respect to the loading: a conservative, a moderate and a radical. The conservative scenario presents an average loading and not rigorous operational limits. The moderate scenario presents a loading 20% higher than the conservative one but the operational limits are higher as well. Finally the radical scenario presents the same loading as the moderate, but the operational limits from the conservative scenario. The machine's cost functions are not changed in any form from one scenario to the other.

5.3 General Aspects of the Numerical Techniques

In this section the description of each system is carried out. The experiments and their numerical results for all the study cases and scenarios are presented. Finally, result discussions about the simulations is assessed, highlighting the points of interest for each system.

The holomorphic embedding method was applied to solve the constrained EDP in the three systems and scenarios. The Newton-Raphson method was used as the base method to validate the results concerning the HEM-EDP.

The simulations were performed starting by the computation of the germ (seed) solution for the HEM-EDP approach. This result was obtained by solving the lossless EDP. The information was also used as guess for the NR method. Following, the residue (mismatch) for the germ solution is calculated and used in the holomorphic embedding process, as detailed in the Chapter 4.

The solution for the lossless EDP was checked before starting the main computations based on HEM-EDP or NR approach. This procedure is to verify whether the operational limits of the generation units are met. In case of fail, the violated limits are activated, suggesting the insertion of respective slack-variables. Once detected an activation of limit, the respective unit generation output power is set at the violated limit and it is kept constant along the HEM-EDP or NR solution calculation. When these approaches reach the convergence, the respective slack-variables associated to violated limits are computed. After this, the algorithm needs to check again whether or not if all limits are met and all slack-variables are positive. In case of fail on this condition, new computations using HEM-EDP or NR approach must be performed. Before, it must be verified possible new limits violations and whether any slack-variable is negative.

In case of negative value of a slack-variable, the violated limit must be relaxed and the power output comes back to be unknown and must be re-calculated by applying again the HEM-EDP or NR approach. The process of using the HEM-EDP or NR approaches continues until convergence is verified and all variables meet their operational limits.

On the simulations concerning the HEM-EDP, the degree of the Taylor's power series was (truncated) limited to $n = 9$. Contributions above this value give very low impact on the results. However, the result for the variables with the approximation of the series up to this degree can stagnate at an unacceptable solution. Certainly, such result justifies to employ the restarted strategy for the HEM, as detailed in the Chapter 4.

The truncation until the 9th degree of the power series allows generation of Padé fractions at most with degree 4 in the numerator and 5 in the denominator (i.e., when the degree of the numerator is different of the denominator, this latter has 1 degree higher). The restarted HEM is adopted in this work. Then the constrain is also applied for all restarts, when this strategy is necessary.

The convergence control was verified by the value of the mismatch of the holomorphic embedding expression presented in the Chapter 4. A tolerance of 10^{-8} was required. The main objective is to demonstrate the performance of the HEM-EDP approach. This performance is observed computing the results of the system variables and monitoring the absolute deviation of the HEM-EDP and NR method.

5.4 Experiments and Results

In this section the data of the system models are presented and verified the results of simulations in different system operational conditions. The power base adopted for all system is 100 MVA.

5.4.1 System 1

The 3-bus system was modeled according to the following parameters for fuel cost and thermal unit heat curve presented respectively at Table 5.1 and Table 5.2.

Table 5.1: Fuel price in \$/MBTU for the system 1

Unit Number	Bus 1	Bus 2
1	1.03	0.97
2	0.97	1.01
3	-	1.00

The impedance of the transmission line connecting buses 1, 2 and 3 are in pu on the 100 MVA base. The following information was used: $z_{13} = 0.10 + j0.7$ pu and $z_{23} = 0.1 + j0.6$ pu.

5.4.1.1 Conservative Scenario

For the Conservative Scenario (CS) the operational limits for the generation units are presented in Table 5.3. The loading in MW for each bus is $L_1 = 50$, $L_2 = 80$ and $L_3 = 40$.

Table 5.2: Heat curve parameters for thermal units in MBTU/h of the system 1

Parameter	Unit Number	Bus 1	Bus 2
h_1	1	0.00142	0.00122
	2	0.00142	0.00142
	3	-	0.00132
h_2	1	0.0142	0.0152
	2	0.0142	0.0142
	3	-	0.0142
h_3	1	0.12	0.13
	2	0.12	0.12
	3	-	0.13

Table 5.3: Operational Limits CS, in pu

Unit Number	Bus 1	Bus 2	Bus 1	Bus 2
	Lower Limit(pu)		Upper Limit(pu)	
1	0.03	0.03	0.5	0.5
2	0.03	0.03	0.55	0.5
3	-	0.03	-	0.5

Applying these conditions and using the data for the system 1, the results for the HEM-EDP and NR methods are depicted in Table 5.4. The notation for the values of P_i (vector whose entries are elements of the table column) in the table is related to the power output of the thermal units, according to the number of units connected to a generation bus. In this sense, for the two power generation connected at buses 1 and 2, $P_{1j} = P_i(1 : j)$, $j = 1 : 2$ and $P_{2j} = P_i(3 : 5)$, $j = 1 : 3$. The values of λ_i are related to the Lagrangean multiplier for each bus. The values for θ_i refers to the phase angles θ_2 and θ_3 , when $\theta_1 = 0$. The slack-variable values are associated to the violated limits. The two generation units at bus 1 had their upper operational limits violated. Therefore, the values exhibited in the table are interpreted as $\bar{\pi}_{11} = 0.1724 \times 10^{-3}$ and $\bar{\pi}_{12} = 0.4990 \times 10^{-3}$.

Table 5.4: Economic Dispatch Results System 1 CS

	HEM No Limits(pu)	HEM Limits(pu)	NR No Limits(pu)	NR Limits(pu)
P_i	0.4622	0.5000	0.4622	0.5000
	0.6261	0.5500	0.6261	0.5500
	0.2978	0.3124	0.2978	0.3124
	0.3859	0.3980	0.3859	0.3980
	0.4730	0.4862	0.4730	0.4862
λ_i	0.0160	0.0163	0.0160	0.0163
	0.0154	0.0155	0.0154	0.0155
	0.0173	0.0174	0.0173	0.0174
θ_i	0.0620	0.1116	0.0620	0.1116
	-0.2720	-0.2457	-0.2720	-0.2457
π_i	-	0.1724×10^{-3}	-	0.1724×10^{-3}
	-	0.4990×10^{-3}	-	0.4990×10^{-3}

From the results presented at Table 5.4, it is interesting to notice that even though machine number 1 had not initially violated its operational limit, the final result for the system restricted its power output to the maximum value. This is due to the fact that at each limit violation, the unit is set to the violated limit and its lagrangian multiplier (π_i) is calculated. By setting unit 2 to its limit and calculating the system new solution, machine 1 has also extrapolated its limit. Thus for a final solution, both units were set to their maximum operating limits.

The accuracy of the methods was also verified. The results are presented in Fig.

5.4. However, the term iteration is attributed to the NR method only. When the HEM-EDP is analyzed, the interpretation for the term 'iteration' in the plot must be understood as 'restart'. It is possible to notice that at every reinitialization of the method, the HEM-EDP has its accuracy improved. The NR method also presents improvements on the reduction of the mismatch. Even so, the HEM approach presents a better result than the NR method. This superiority in precision is evidenced by the fact that the HEM-EDP only needed one restart to achieve the desired accuracy of 10^{-15} , while the NR method needed two iterations to meet the tolerance 10^{-8} .

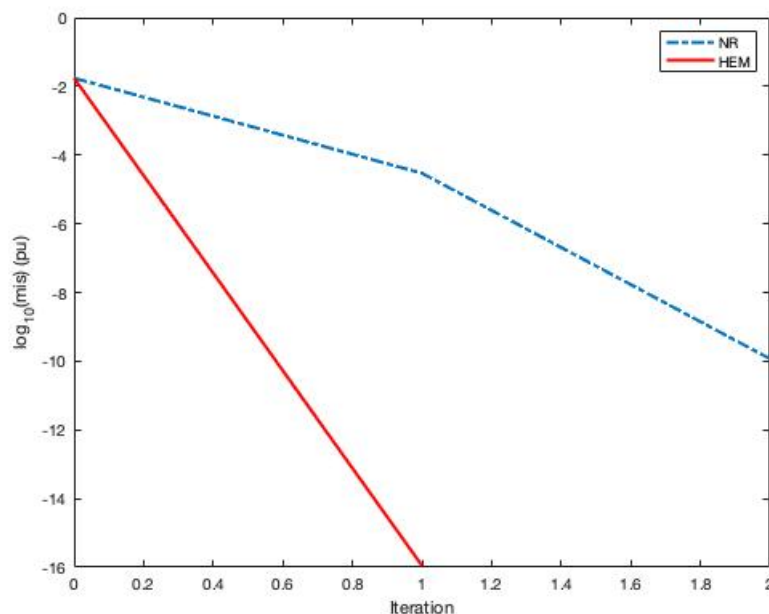


Figure 5.4: Comparative Solution Error System 1 CS

5.4.1.2 Moderate Scenario

For the Moderate Scenario (MS), the loading and operational limits presented in Table 5.5 and Table 5.6, respectively, were adopted.

Applying these conditions for the system 1, the results for the HEM-EDP and NR method were the following depicted in Table 5.7:

Analyzing the results presented at Table 5.7, it can be noticed that even though machine number 2 had initially violated its operating limit, its configuration to its maximum power output did not drive any other unit to its limit like in the conservative

Table 5.5: Operational Limits MS

Unit Number	Bus 1	Bus 2	Bus 1	Bus 2
	Lower Limit(pu)		Upper Limit(pu)	
1	0.03	0.03	0.6	0.6
2	0.03	0.03	0.65	0.6
3	-	0.03	-	0.6

Table 5.6: System Loading MS

Bus Number	P	Q
1	60.0	0.0
2	96.0	0.0
3	48.0	36.0

Table 5.7: Economic Dispatch Results System 1 MS

	HEM No Limits(pu)	HEM Limits(pu)	NR No Limits(pu)	NR Limits(pu)
P_i	0.5483	0.5948	0.5483	0.5948
	0.7148	0.6500	0.7148	0.6500
	0.3651	0.3721	0.3651	0.3721
	0.4414	0.4472	0.4414	0.4472
	0.5333	0.5396	0.5333	0.5396
λ_i	0.0162	0.0164	0.0162	0.0164
	0.0156	0.0156	0.0156	0.0156
	0.0178	0.0179	0.0178	0.0179
θ_i	0.0707	0.0942	0.0707	0.0942
	-0.3233	-0.3108	-0.3233	-0.3108
π_i	-	0.3198 10^{-3}	-	0.3198 10^{-3}

scenario. This is due to the fact that when the loading was elevated from one scenario to the other, so were the limits. Yielding in a final solution with only one unit operating at its limit.

The accuracy of the methods was once again observed. The results are presented in Fig. 5.5. Once more, it can be noticed that at every reinitialization of the method, both NR and HEM have their accuracy improved with the HEM presenting always a better result than the NR method.

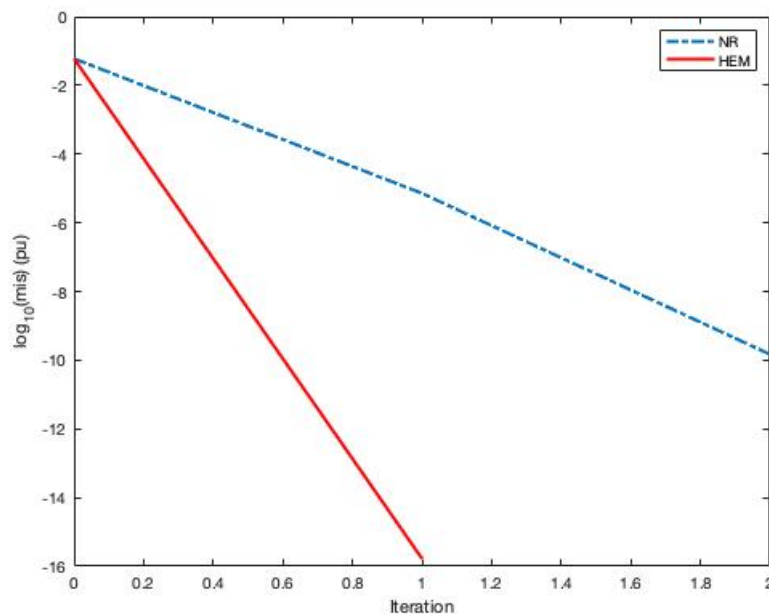


Figure 5.5: Comparative Solution Error System 1 MS

5.4.1.3 Radical Scenario

For the Radical Scenario (RS), the loading and operational limits presented in Table 5.8 and Table 5.9 respectively, were adopted.

Applying these conditions for the system 1, the results for the HEM and NR methods were the following depicted in Table 5.10:

From the data at Table 5.4, it is observed that the overall system behavior is very similar to the conservative scenario, with machine number 1 not initially violating its operating limit and the final result for the system restricting its power output to the

Table 5.8: Operating Limits RS

Unit Number	Bus 1	Bus 2	Bus 1	Bus 2
	Lower Limit(pu)		Upper Limit(pu)	
1	0.03	0.03	0.6	0.6
2	0.03	0.03	0.6	0.6
3	-	0.03	-	0.6

Table 5.9: System Loading RS

Bus Number	P	Q
1	60.0	0.0
2	96.0	0.0
3	48.0	36.0

Table 5.10: Economic Dispatch Results System 1 RS

	HEM No Limits(pu)	HEM Limits(pu)	NR No Limits(pu)	NR Limits(pu)
P_i	0.5483	0.6000	0.5483	0.6000
	0.7148	0.6000	0.7148	0.6000
	0.3651	0.3895	0.3651	0.3895
	0.4414	0.4615	0.4414	0.4615
	0.5333	0.5552	0.5333	0.5552
λ_i	0.0162	0.0167	0.0162	0.0167
	0.0156	0.0157	0.0156	0.0157
	0.0178	0.0181	0.0178	0.0181
θ_i	0.0707	0.1521	0.0707	0.1521
	-0.3233	-0.2801	-0.3233	-0.2801
π_i	-	$0.3244 \cdot 10^{-3}$	-	$0.3244 \cdot 10^{-3}$
	-	$0.8015 \cdot 10^{-3}$	-	$0.8015 \cdot 10^{-3}$

maximum value. This was due to the fact that at each limit violation, the unit is set to the violated limit and its lagrangean multiplier (π_i) is calculated. By setting unit 2 to its limit and calculating the system new solution, machine 1 also extrapolated its limit. Thus, for a final solution both units were set to their maximum operating limits.

Once more the methods accuracy was verified. The results are presented in Fig. 5.6. Once more, the HEM at every reinitialization of the method, had a better result than the NR for the same initial guess.

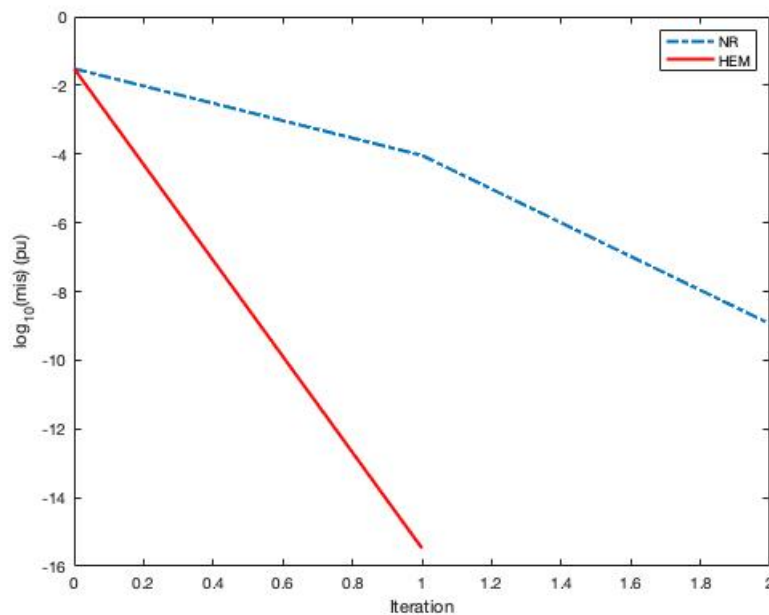


Figure 5.6: Comparative Solution Error System 1 RS

Comparing the three scenarios, it is evident that the change in loading and operational limits did not affect the overall economical balance. The unit 2 being, regardless of loading, the most demanded unit followed by unit 1, and with unit 3 being the last demanded unit in all scenarios. It is visible also an homogeneity in the system. Even though unit 3 is always less demanded than the rest, its power output does not fall below the operating limits.

5.4.2 System 2

The nine bus system studied was modelled according to the following parameters for fuel cost and thermal units heat curve presented respectively at Table 5.11 and

Table 5.12.

Table 5.11: Fuel Cost System 2

Unit Number	Bus 1	Bus 2	Bus 3
1	1.03	0.97	1.02
2	1.00	1.01	1.03
3	-	1.00	1.00

Table 5.12: Heat Curve Parameters System 2

Parameter	Unit Number	Bus 1	Bus 2	Bus 3
H_1	1	0.00142	0.00122	0.00152
	2	0.00142	0.00142	0.00112
	3	-	0.00132	0.00150
H_2	1	0.0142	0.0152	0.0122
	2	0.0142	0.0142	0.0132
	3	-	0.0142	0.0130
H_3	1	0.12	0.13	0.11
	2	0.12	0.12	0.10
	3	-	0.13	0.10

The impedances for the transmission lines and its connections were the ones found in the IEEE 9-bus system. No modification was made in terms of connections and its values.

5.4.2.1 Conservative Scenario

For the Conservative Scenario (CS) the operational limits presented in Table 5.13, were adopted. The loading in MW for each bus is $L_5 = 90$, $L_7 = 100$ and $L_9 = 125$.

Applying these conditions on the system 2 the results for the HEM and NR methods, obtained in the MATLAB, were the following depicted in Table 5.14. Note that the same method as before was used for exposing the results, i.e. for the two power generation connected to buses 1, 2 and 3, $P_{1j} = P_i(1 : j)$, $j = 1 : 2$, $P_{2j} = P_i(3 : 5)$, $j = 1 : 3$ and $P_{3j} = P_i(6 : 8)$, $j = 1 : 3$.

Table 5.13: Operating Limits CS

Unit	Bus 1	Bus 2	Bus 3	Bus 1	Bus 2	Bus 3
	Lower Limit			Upper Limit		
1	0.05	0.05	0.3	0.3	0.2	0.9
2	0.05	0.1	0.3	0.35	0.4	0.6
3	-	0.1	0.3	-	0.4	0.8

Table 5.14: Economic Dispatch Results System 2 CS

	HEM No Limits	HEM Limits	NR No Limits	NR Limits
P_i	0.3671	0.3000	0.3671	0.3000
	0.5281	0.3500	0.5281	0.3500
	0.2088	0.3407	0.2088	0.3407
	0.3124	0.2641	0.3124	0.2641
	0.3932	0.3407	0.3932	0.3407
	0.8346	0.7368	0.8346	0.7368
	0.9548	0.4910	0.9548	0.4910
	-0.4064	0.5763	-0.4064	0.5763
λ_i	0.0157	0.0157	0.0157	0.0157
	0.0152	0.0151	0.0152	0.0151
	0.0150	0.0147	0.0150	0.0147
	0.0157	0.0157	0.0157	0.0157
	0.0158	0.0157	0.0158	0.0155
	0.0150	0.0147	0.0150	0.0147
	0.0153	0.0151	0.0153	0.0151
	0.0152	0.0151	0.0152	0.0151
	0.0159	0.0158	0.0159	0.0158
θ_i	0.0515	0.0701	0.0515	0.0701
	0.1256	0.2170	0.1256	0.2170
	-0.0516	-0.0374	-0.0516	-0.0374
	-0.0747	-0.0427	-0.0747	-0.3167
	0.0446	0.1113	0.0446	0.1113
	-0.0274	0.0169	-0.0274	0.0169
	-0.0056	0.0229	-0.0056	0.0229
	-0.1075	-0.0886	-0.1075	-0.0886
	π_i	-	$0.1779 \cdot 10^{-3}$	-
-		$0.4875 \cdot 10^{-3}$	-	$0.4875 \cdot 10^{-3}$

The data from Table 5.14, presents machine number 8 initially with a negative power output. This indicates that without any consideration for the electrical point of view of the system this machine is too expensive. Therefore, from an purely mathematical point of view, the negative output indicates that instead of generating costs the machine is generating revenue.

Other relevant aspect to take into consideration is the high number of violating units in the original solution, units 1, 2, 3 and 7 are above the upper limits. This is mostly caused by the negative output for machine number 8. Once all limits are set and their lagrangian multipliers (π_i) calculated a verification is done. Case there are any π_i values bellow zero this limits are removed. The final solution presented units 1 and 2 at the minimum output and unit 6 presenting the higher power output for the system. A very different result from the limitless system.

The methods accuracy continued to be simulated in MATLAB. The results are presented in Fig. 5.7. Again, the better accuracy for the HEM over the NR is verified, with the later needing only one restart and the other two iterations for achieving the specified tolerance.

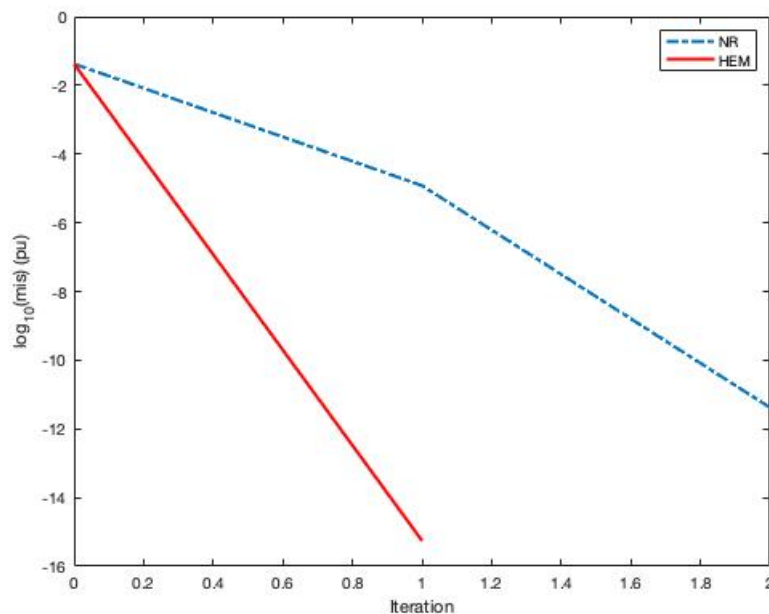


Figure 5.7: Comparative Solution Error System 2 CS

5.4.2.2 Moderate Scenario

For the Moderate Scenario (MS) the loading and operational limits presented in Table 5.15 and Table 5.16 respectively, were adopted.

Table 5.15: Operating Limits MS

Unit	Bus 1	Bus 2	Bus 3	Bus 1	Bus 2	Bus 3
	Lower Limit			Upper Limit		
1	0.05	0.05	0.3	0.35	0.25	1.1
2	0.05	0.1	0.3	0.4	0.5	0.75
3	-	0.1	0.3	-	0.5	0.95

Table 5.16: System Loading MS

Bus Number	P	Q
1	0.0	0.0
2	0.0	0.0
3	0.0	0.0
4	0.0	0.0
5	108.0	36.0
6	0.0	0.0
7	120.0	42.0
8	0.0	0.0
9	150.0	60.0

Applying these conditions on the system 2 the results for the HEM and NR methods, obtained in the MATLAB, were the following depicted in Table 5.17:

Analyzing Table 5.17, is possible to notice that machine number 8, once more, initially presented a negative power output. This indicates that even though the loading in the system was altered, from the mathematical point of view of the system this machine continues to be too expensive. Therefore the negative output indicates that instead of generating costs the machine is generating revenue, creating thus an overall less expensive solution.

Other important aspect to take into consideration is the shift of violating units from the original solution to the final solution yielding in units 1, 2, 3 and 7 above the

Table 5.17: Economic Dispatch Results System 2 MS

	HEM No Limits	HEM Limits	NR No Limits	NR Limits
P_i	0.4690	0.3500	0.4690	0.3500
	0.6331	0.4000	0.6331	0.4000
	0.2942	0.2500	0.2942	0.2500
	0.3829	0.3555	0.3829	0.3555
	0.4698	0.4400	0.4698	0.4400
	0.8964	0.8152	0.8964	0.8192
	1.0421	0.5963	1.0421	0.5963
	-0.3479	0.6572	-0.3479	0.6572
λ_i	0.0160	0.0161	0.0160	0.0161
	0.0154	0.0154	0.0154	0.0154
	0.0152	0.0150	0.0152	0.0150
	0.0160	0.0161	0.0160	0.0161
	0.0162	0.0162	0.0162	0.0162
	0.0152	0.0150	0.0152	0.0150
	0.0155	0.0154	0.0155	0.0154
	0.0154	0.0154	0.0154	0.0154
	0.0162	0.0163	0.0162	0.0163
θ_i	0.0638	0.1064	0.0638	0.1064
	0.1378	0.2530	0.1378	0.2530
	-0.0635	-0.0432	-0.0635	-0.0432
	-0.0939	-0.0509	-0.0939	-0.0509
	0.0445	0.1318	0.0445	0.1318
	-0.0373	0.0275	-0.0373	0.0275
	-0.0078	0.0411	-0.0078	0.0411
	-0.1306	-0.1007	-0.1306	-0.1007
π_i	-	0.4801 10^{-3}	-	0.4801 10^{-3}
	-	0.7939 10^{-3}	-	0.7939 10^{-3}
	-	0.0259 10^{-3}	-	0.0259 10^{-3}

upper limit. This is mostly caused by the negative output for machine number 8. The final solution presented only units 1, 2 and 3 at their maximum output with unit 6 presenting the higher power output for the system. A different result from the limitless system.

For the solution accuracy the results in Fig. 5.8 show once more the same overall behavior for the HEM and NR, the later with a superior accuracy for the same initial guess and needing less restarts for achieving the especified tolerance.

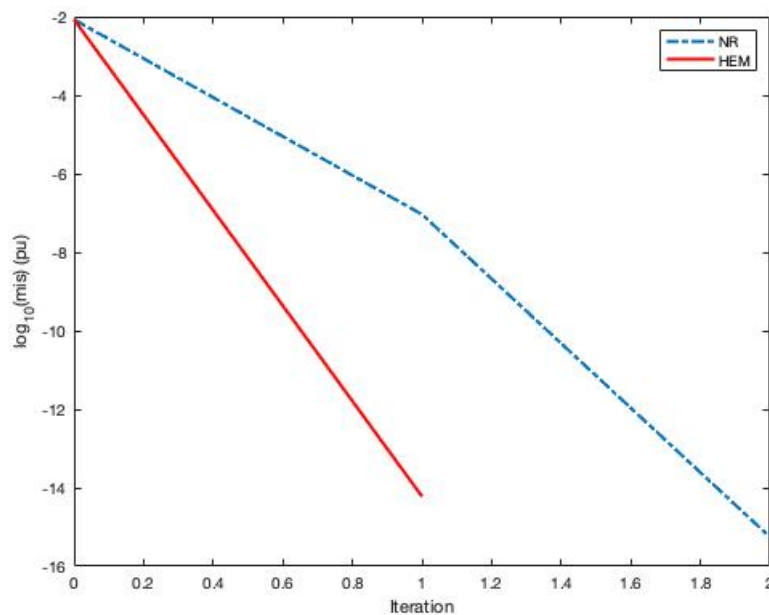


Figure 5.8: Comparative Solution Error System 2 MS

5.4.2.3 Radical Scenario

For the Radical Scenario (RS) the loading and operational limits presented in Table 5.18 and Table 5.19 respectively, were adopted.

Applying these conditions on the system 2 the results for the HEM and NR methods, obtained in the MATLAB, were the following depicted in Table 5.20:

On Table 5.20, can be verified that machine number 8, continues, for the limitless solution, to present a negative power output. This demonstrates that eventhough the

Table 5.18: Operating Limits RS

Unit	Bus 1	Bus 2	Bus 3	Bus 1	Bus 2	Bus 3
	Lower Limit			Upper Limit		
1	0.05	0.05	0.3	0.3	0.2	0.9
2	0.05	0.1	0.3	0.35	0.4	0.6
3	-	0.1	0.3	-	0.4	0.8

Table 5.19: System Loading RS

Bus Number	P	Q
1	0.0	0.0
2	0.0	0.0
3	0.0	0.0
4	0.0	0.0
5	108.0	36.0
6	0.0	0.0
7	120.0	42.0
8	0.0	0.0
9	150.0	60.0

Table 5.20: Economic Dispatch Results System 2 RS

	HEM No Limits	HEM Limits	NR No Limits	NR Limits
P_i	0.4690	0.3000	0.4690	0.3000
	0.6331	0.3500	0.6331	0.3500
	0.2942	0.2000	0.2942	0.2000
	0.3829	0.4000	0.3829	0.4000
	0.4698	0.4000	0.4698	0.4000
	0.8964	0.8895	0.8964	0.8895
	1.0421	0.6000	1.0421	0.6000
	-0.3479	0.7341	-0.3479	0.7341
λ_i	0.0160	0.0165	0.0160	0.0165
	0.0154	0.0157	0.0154	0.0157
	0.0152	0.0152	0.0152	0.0152
	0.0160	0.0165	0.0160	0.0165
	0.0162	0.0165	0.0162	0.0165
	0.0152	0.0152	0.0152	0.0152
	0.0155	0.0157	0.0155	0.0157
	0.0154	0.0157	0.0154	0.0157
	0.0162	0.0167	0.0162	0.0167
θ_i	0.0638	0.1165	0.0638	0.1265
	0.1378	0.2882	0.1378	0.2882
	-0.0635	-0.0374	-0.0635	-0.0374
	-0.0939	-0.0383	-0.0939	-0.0383
	0.0445	0.1579	0.0445	0.1579
	-0.0373	0.0459	-0.0373	0.0459
	-0.0078	0.0540	-0.0078	0.0540
	-0.1306	-0.0925	-0.1306	-0.0925
π_i	-	0.0010 10^{-3}	-	0.0010 10^{-3}
	-	0.0013 10^{-3}	-	0.0013 10^{-3}
	-	0.0004 10^{-3}	-	0.0004 10^{-3}
	-	0.0002 10^{-3}	-	0.0002 10^{-3}
	-	0.0004 10^{-3}	-	0.0004 10^{-3}
	-	0.0002 10^{-3}	-	0.0002 10^{-3}

limits and loading being altered the overall system balance is kept, and unit 8 is still too expensive.

Other important aspect to take into consideration is the how the violating units from the original solution to the final solution did not changed. Units 1, 2, 3, 4, 5 and 7 were above the upper limit in the limitless scenario. This was mostly caused by the negative output for machine number 8. The final solution presented the same units 1, 2, 3, 4, 5 and 7 at their maximum output and unit 6 presenting the higher power output for the system.

The accuracy of the methods as presented in Fig. 5.9 does not suffer any significant changes. The HEM continues to have a superior performance when compared to NR.

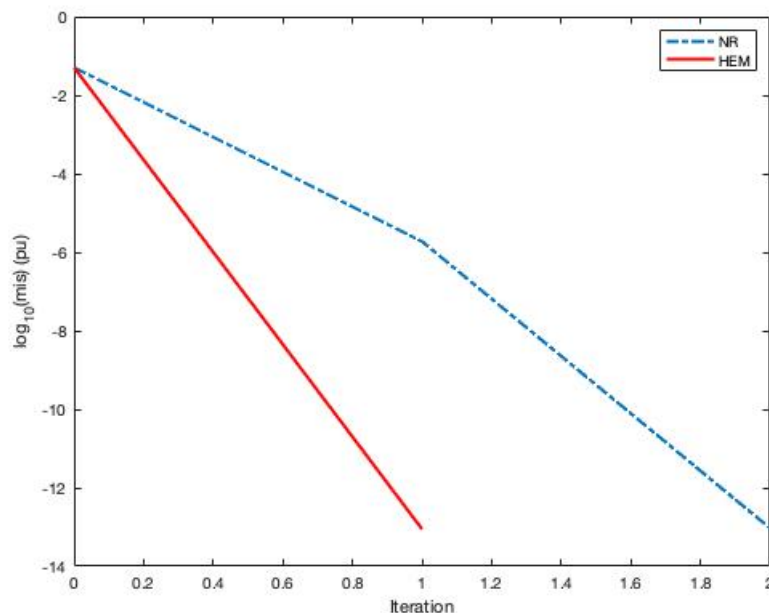


Figure 5.9: Comparative Solution Error System 2 RS

Comparing the three scenarios is evident that the change in loading and operational limits did not affect the overall system balance, with unit 6 being regardless of loading the most demanded unit and with units 1 and 2 always at their upper limits in all scenarios. It is also evident the great impact that a more expensive unit cause in the system, throwing several units to their limits for compensating the expensive machine, even though this might generate more losses.

5.4.3 System 3

The fourteen bus system studied was modelled according to the following parameters for fuel cost and thermal units heat curve presented respectively at Table 5.21 and Table 5.22.

Table 5.21: Fuel Cost System 3

Unit Number	Bus 1	Bus 2	Bus 3	Bus 6	Bus 8
1	1.03	0.97	1.03	0.97	1.02
2	1.00	1.01	1.00	1.01	0.98
3	0.98	1.00	-	-	1.01

Table 5.22: Heat Curve Parameters System 3

Parameter	Unit Number	Bus 1	Bus 2	Bus 3	Bus 6	Bus 8
H_1	1	0.00142	0.00122	0.00142	0.00152	0.00122
	2	0.00142	0.00142	0.00142	0.00142	0.00132
	3	0.00152	0.00132	-	-	0.00162
H_2	1	0.0142	0.0152	0.0142	0.0152	0.0122
	2	0.0142	0.0142	0.0142	0.0142	0.0132
	3	0.0142	0.0142	-	-	0.0162
H_3	1	0.12	0.13	0.12	0.13	0.11
	2	0.12	0.12	0.12	0.12	0.10
	3	0.11	0.13	-	-	0.12

The impedances for the transmission lines and its connections were the ones found in the IEEE 14-bus system. No modification was made in terms of connections and its values.

5.4.3.1 Conservative Scenario

For the Conservative Scenario (CS) the operational limits presented in Table 5.23, were adopted. The loading in MW for each bus is $L_2 = 21.7$, $L_3 = 94.2$, $L_4 = 47.8$, $L_5 = 7.6$, $L_6 = 11.2$, $L_9 = 29.5$, $L_{10} = 9$, $L_{11} = 3.5$, $L_{12} = 6.1$, $L_{13} = 13.5$ and $L_{14} = 14.9$.

Table 5.23: Operating Limits CS

Unit	Bus 1	Bus 2	Bus 3	Bus 6	Bus 8	Bus 1	Bus 2	Bus 3	Bus 6	Bus 8
	Lower Limit					Upper Limit				
1	0.05	0.05	0.05	0.03	0.3	0.4	0.3	0.3	0.3	0.9
2	0.1	0.05	0.05	0.1	0.3	0.4	0.5	0.5	0.3	0.9
3	0.1	0.05	-	-	0.1	0.6	0.5	-	-	0.4

Applying these conditions on the system 3 the results for the HEM and NR methods, obtained in the MATLAB, were the following depicted in Table 5.24. Note that the same scheme was used for exposing the results, i.e. for the two power generation connected to buses 1, 2, 3, 6 and 8, $P_{1j} = P_i(1 : j)$, $j = 1 : 3$, $P_{2j} = P_i(4 : 6)$, $j = 1 : 3$, $P_{3j} = P_i(7 : 8)$, $j = 1 : 2$, $P_{6j} = P_i(9 : 10)$, $j = 1 : 2$ and $P_{8j} = P_i(11 : 13)$, $j = 1 : 3$.

Analyzing Table 5.24, is verified that machines numbers 1 and 13 initially presented a negative power output. Once more this result indicates that, from a mathematical point of view of the system, these machines are too expensive, therefore operating in a motor manner they would not generate cost but revenue. This is not true in reality thus the need for operational limits.

Other important aspect to take into consideration is how the violating units from the original solution to the final solution increased. Unit 4 was the only bellow the lower limit in the original solution. The final solution presented units 1, 2, 4, 9 and 13 at the minimum output and unit 12 presenting the higher power output for the system.

The accuracy verification presented encore the HEM with a better performance than the NR method for the same initial conditions, achieving the imposed precision with less restarts than the number of needed iterations.

5.4.3.2 Moderate Scenario

For the Conservative Scenario (CS) the loading and operational limits presented in Table 5.25 and Table 5.26 respectively, were adopted.

Applying these conditions on the system 3 the results for the HEM and NR

Table 5.24: Economic Dispatch Results System 3 CS

	HEM No Limits	HEM Limits	NR No Limits	NR Limits
P_i	-0.0132	0.0500	-0.0132	0.0500
	0.1364	0.1000	0.1364	0.1000
	0.2254	0.1591	0.2254	0.1591
	0.0017	0.0500	0.0017	0.0500
	0.1416	0.0778	0.1416	0.0778
	0.2076	0.1383	0.2076	0.1383
	0.1956	0.1530	0.1956	0.1530
	0.3515	0.3076	0.3515	0.3076
	0.0800	0.0300	0.0800	0.0300
	0.2061	0.1240	0.2061	0.1240
	0.7429	0.6414	0.7429	0.6414
	0.8253	0.6819	0.8253	0.6819
	-0.4933	0.1000	-0.4933	0.1000
λ_i	0.0146	0.0144	0.0146	0.0144
	0.0147	0.0146	0.0147	0.0146
	0.0152	0.0151	0.0152	0.0151
	0.0149	0.0147	0.0149	0.0147
	0.0147	0.0144	0.0147	0.0144
	0.0149	0.0146	0.0149	0.0146
	0.0149	0.0146	0.0149	0.0146
	0.0149	0.0146	0.0149	0.0146
	0.0148	0.0146	0.0148	0.0146
	0.0149	0.0147	0.0149	0.0147
	0.0150	0.0147	0.0150	0.0147
	0.0152	0.0149	0.0152	0.0149
	0.0153	0.0150	0.0153	0.0150
	0.0154	0.0151	0.0154	0.0151
θ_i	-0.0173	-0.0148	-0.0173	-0.0148
	-0.0706	-0.0781	-0.0706	-0.0781
	-0.0424	-0.0386	-0.0424	-0.0386
	-0.0197	-0.0064	-0.0197	-0.0064
	-0.1907	-0.1804	-0.1907	-0.1804
	-0.1304	-0.1250	-0.1304	-0.1250
	-0.1304	-0.1250	-0.1304	-0.1250
	-0.1683	-0.1621	-0.1683	-0.1621
	-0.1808	-0.1739	-0.1808	-0.1739
	-0.1897	-0.1811 ⁷²	-0.1897	-0.1811

	HEM No Limits	HEM Limits	NR No Limits	NR Limits
θ_i	-0.2113	-0.2013	-0.2113	-0.2013
	-0.2132	-0.2036	-0.2132	-0.2036
	-0.2159	-0.2082	-0.2159	-0.2082
π_i	-	$0.4000 \cdot 10^{-3}$	-	$0.4000 \cdot 10^{-3}$
	-	$0.1000 \cdot 10^{-3}$	-	$0.1000 \cdot 10^{-3}$
	-	$0.3000 \cdot 10^{-3}$	-	$0.3000 \cdot 10^{-3}$
	-	$0.1000 \cdot 10^{-3}$	-	$0.0100 \cdot 10^{-3}$
	-	$2.3000 \cdot 10^{-3}$	-	$2.3000 \cdot 10^{-3}$

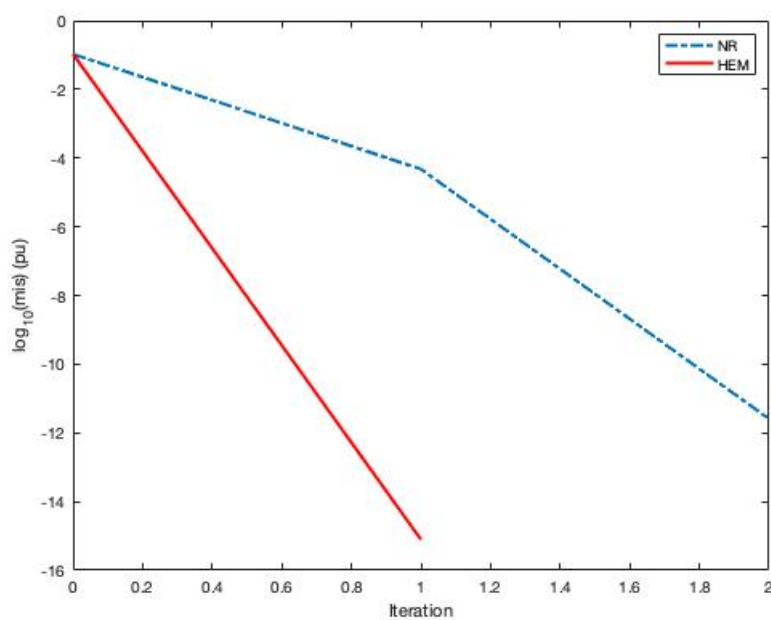


Figure 5.10: Comparative Solution Error System 3 CS

Table 5.25: Operating Limits MS

Unit	Bus 1	Bus 2	Bus 3	Bus 6	Bus 8	Bus 1	Bus 2	Bus 3	Bus 6	Bus 8
	Lower Limit					Upper Limit				
1	0.1	0.1	0.1	0.05	0.35	0.5	0.35	0.35	0.35	1.1
2	0.15	0.1	0.1	0.15	0.35	0.5	0.6	0.6	0.35	1.1
3	0.15	0.1	-	-	0.15	0.75	0.6	-	-	0.5

Table 5.26: System Loading MS

Bus Number	P	Q
1	0.0	0.0
2	26.0	15.2
3	113	22.8
4	57.4	-4.7
5	9.2	1.9
6	13.4	9.0
7	0.0	0.0
8	0.0	0.0
9	35.4	20
10	10.8	7.0
11	4.2	2.2
12	7.3	1.9
13	16.2	7.0
14	17.9	6.0

methods, obtained in the MATLAB, were the following depicted in Table 5.27:

Evaluating Table 5.27, it can be noticed that the increase on the system loading made only machine number 13 to initially present a negative power output. Instead of the conservative system were machines 1 and 13 presented negatives outputs.

Another aspect to take into consideration is how the violating units from the limitless run to the final solution increased. Units 1 and 4 were the only ones bellow the lower treshold in the free limits solution. However in the final solution units 1, 2, 4, 9 and 13 presented themselves at their minimum output and unit 12 presented the higher power output of the system. This was the same machine arrangement as the on in the conservative scenario.

The precision verification presented still the HEM with a better performance than the NR method for the same initial conditions, achieving the imposed precision with less restarts than the number of needed iterations.

Table 5.27: Economic Dispatch Results System 3 MS

	HEM No Limits	HEM Limits	NR No Limits	NR Limits
P_i	0.0090	0.1000	0.0090	0.1000
	0.1593	0.1500	0.1593	0.1500
	0.2472	0.1686	0.2472	0.1686
	0.0391	0.1000	0.0391	0.1000
	0.1724	0.1016	0.1724	0.1016
	0.2411	0.1641	0.2411	0.1641
	0.2554	0.2101	0.2554	0.2101
	0.4131	0.3664	0.4131	0.3664
	0.1373	0.0500	0.1373	0.0500
	0.2534	0.1707	0.2534	0.1707
	0.7816	0.6763	0.7816	0.6763
	0.8799	0.7312	0.8799	0.7312
	-0.4567	0.1500	-0.4567	0.1500
λ_i	0.0147	0.0144	0.0147	0.0144
	0.0148	0.0146	0.0148	0.0146
	0.0154	0.0152	0.0154	0.0152
	0.0151	0.0148	0.0151	0.0148
	0.0149	0.0145	0.0149	0.0145
	0.0150	0.0147	0.0150	0.0147
	0.0150	0.0147	0.0150	0.0147
	0.0150	0.0147	0.0150	0.0147
	0.0149	0.0147	0.0149	0.0147
	0.0151	0.0148	0.0152	0.0148
	0.0151	0.0148	0.0152	0.0148
	0.0154	0.0151	0.0154	0.0151
	0.0155	0.0152	0.0155	0.0152
	0.0157	0.0154	0.0157	0.0154
θ_i	-0.0199	-0.0229	-0.0199	-0.0229
	-0.0830	-0.0941	-0.0830	-0.0941
	-0.0508	-0.0512	-0.0508	-0.0512
	-0.0261	-0.0160	-0.0261	-0.0160
	-0.2307	-0.2239	-0.2307	-0.2239
	-0.1570	-0.1557	-0.1570	-0.1557
	-0.1570	-0.1557	-0.1570	-0.1557
	-0.2028	-0.2005	-0.2028	-0.2005
	-0.2180	-0.2149	-0.2180	-0.2149
	-0.2291	-0.2242 ⁷⁵	-0.2291	-0.2242

	HEM No Limits	HEM Limits	NR No Limits	NR Limits
θ_i	-0.2555	-0.2489	-0.2555	-0.2489
	-0.2577	-0.2516	-0.2577	-0.2516
	-0.2605	-0.2566	-0.2605	-0.2566
π_i	-	$0.5000 \cdot 10^{-3}$	-	$0.5000 \cdot 10^{-3}$
	-	$0.2000 \cdot 10^{-3}$	-	$0.2000 \cdot 10^{-3}$
	-	$0.3000 \cdot 10^{-3}$	-	$0.3000 \cdot 10^{-3}$
	-	$0.0900 \cdot 10^{-3}$	-	$0.0900 \cdot 10^{-3}$
	-	$2.3000 \cdot 10^{-3}$	-	$2.3000 \cdot 10^{-3}$

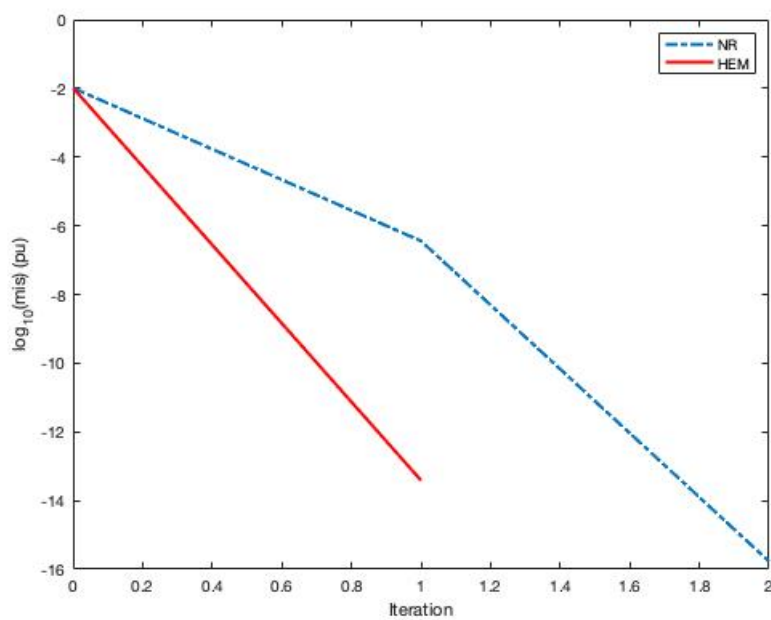


Figure 5.11: Comparative Solution Error System 3 MS

5.4.3.3 Radical Scenario

For the Conservative Scenario (CS) the loading and operational limits presented in Table 5.28 and Table 5.29 respectively, were adopted.

Table 5.28: Operating Limits RS

Unit	Bus 1	Bus 2	Bus 3	Bus 6	Bus 8	Bus 1	Bus 2	Bus 3	Bus 6	Bus 8
	Lower Limit					Upper Limit				
1	0.05	0.05	0.05	0.03	0.3	0.4	0.3	0.3	0.3	0.9
2	0.1	0.05	0.05	0.1	0.3	0.4	0.5	0.5	0.3	0.9
3	0.1	0.05	-	-	0.1	0.6	0.5	-	-	0.4

Table 5.29: System Loading RS

Bus Number	P	Q
1	0.0	0.0
2	26.0	15.2
3	113	22.8
4	57.4	-4.7
5	9.2	1.9
6	13.4	9.0
7	0.0	0.0
8	0.0	0.0
9	35.4	20
10	10.8	7.0
11	4.2	2.2
12	7.3	1.9
13	16.2	7.0
14	17.9	6.0

Applying these conditions on the system 3 the results for the HEM and NR methods, obtained in the MATLAB, were the following depicted in Table 5.30:

From the results presented at Table 5.30, is of note that the same machine as in the moderate scenario initially presented a negative power output. This is due to the fact that both scenarios have the same loading profile.

Table 5.30: Economic Dispatch Results System 3 RS

	HEM No Limits	HEM Limits	NR No Limits	NR Limits
P_i	0.0090	0.0500	0.0090	0.0500
	0.1593	0.1101	0.1593	0.1101
	0.2472	0.2003	0.2472	0.2003
	0.0391	0.0500	0.0391	0.0500
	0.1724	0.1264	0.1724	0.1264
	0.2411	0.1911	0.2411	0.1911
	0.2554	0.2237	0.2554	0.2237
	0.4131	0.3804	0.4131	0.3804
	0.1373	0.0596	0.1373	0.0596
	0.2534	0.1893	0.2534	0.1893
	0.7816	0.6964	0.7816	0.6964
	0.8799	0.7595	0.8799	0.7595
	-0.4567	0.1000	-0.4567	0.1000
λ_i	0.0147	0.0145	0.0147	0.0145
	0.0148	0.0147	0.0148	0.0147
	0.0154	0.0153	0.0154	0.0153
	0.0151	0.0149	0.0151	0.0149
	0.0149	0.0146	0.0149	0.0146
	0.0150	0.0148	0.0150	0.0148
	0.0150	0.0148	0.0150	0.0148
	0.0150	0.0148	0.0150	0.0148
	0.0149	0.0147	0.0149	0.0147
	0.0151	0.0149	0.0151	0.0149
	0.0151	0.0149	0.0151	0.0149
	0.0154	0.0151	0.0154	0.0151
	0.0155	0.0152	0.0155	0.0152
	0.0157	0.0154	0.0157	0.0154
θ_i	-0.0199	-0.0202	-0.0199	-0.0202
	-0.0830	-0.0874	-0.0830	-0.0874
	-0.0508	-0.0462	-0.0508	-0.0462
	-0.0261	-0.0120	-0.0261	-0.0120
	-0.2307	-0.2196	-0.2307	-0.2196
	-0.1570	-0.1508	-0.1570	-0.1508
	-0.1570	-0.1508	-0.1570	-0.1508
	-0.2028	-0.1957	-0.2028	-0.1957
	-0.2180	-0.2102	-0.2180	-0.2102
	-0.2291	-0.2197 ⁸	-0.2291	-0.2197

	HEM No Limits	HEM Limits	NR No Limits	NR Limits
θ_i	-0.2555	-0.2446	-0.2555	-0.2446
	-0.2577	-0.2472	-0.2577	-0.2472
	-0.2605	-0.2519	-0.2605	-0.2519
π_i	-	$0.3000 \cdot 10^{-3}$	-	$0.3000 \cdot 10^{-3}$
	-	$0.2000 \cdot 10^{-3}$	-	$0.2000 \cdot 10^{-3}$
	-	$2.1000 \cdot 10^{-3}$	-	$2.1000 \cdot 10^{-3}$

Other important aspect to take into consideration is the how the violating units from the free limits solution to the final solution did not changed. Units 1 and 4 were the only ones bellow the lower limit in the original solution. The final solution presented units 1, 4 and 13 at the minimum output and unit 12 presenting the higher power output for the system.

The accuracy of the methods was also simulated in MATLAB. The results are presented in Fig. 5.12. Again it is possible to notice that at every reinitialization of the method both NR and HEM have their accuracy improved with the HEM presenting always a better result the the NR method. This superiority in precision is evidenced by the fact that the HEM only needed one restart to achieve the desired accuracy of e^{-15} while the NR method needed two restarts.

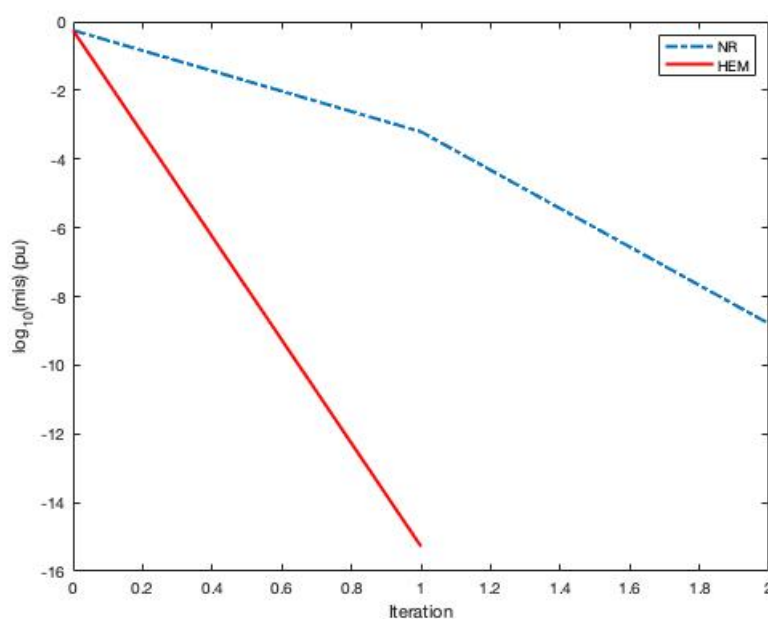


Figure 5.12: Comparative Solution Error System 3 RS

Comparing the three scenarios is evident that the change in loading and operational limits did not affected the overall economical balance, with unit 12 being regardless of loading the most demanded unit and with units 1, 4 and 13 always at theirs lower operational limits in all scenarios. It is present also an homogeneity in the system. This in proven by the fact that changes in the operational limits and loading profiles did not altered the machines typical output distribution.

5.5 Conclusion of this Chapter

In this chapter was presented the results for the HEM applied for Economic Dispatch Problem. It was used three different networks (a generic 3-bus, IEEE 9-bus and IEEE 14-bus) and for each system three different scenarios were considered. All the results were them compared with a solution via Newton-Raphson method. The errors for the two solutions methods were also presented and compared. Finally an overview of the different scenarios was made.

Chapter 6 CONCLUSION

6.1 Conclusion

This work proposed an alternative method for solving the multibus economic dispatch problem for thermal units under a lossy transmission system in power systems. The methodology is based on the holomorphic embedding method. This technique was employed recently for solving the power flow problem. The approach was adapted in this dissertation to solve the lossy EDP. To achieve this goal, a strategy which uses the residue (mismatch) of a nonlinear system to compose the embedding model was adopted. The lossless EDP solution was employed as 'germ solution' to start the HEM problem applied to EDP. This same solution was also employed as estimate for solving the nonlinear problem by the Newton-Raphson method, which is used as reference to evaluate the performance of the proposed method.

A detailed bibliographic survey on the problem of economic dispatch of thermal generating units was performed. Emphasis was given to the search that focused on the static economic dispatch, that is, the one proposed for a given moment, and which is kept constant during the day. For this was the focus of the present dissertation. Also, we sought to highlight the main works that address contributions about HEM.

The formulation of the EDP was discussed in Chapter 2, where its fundamentals were treated. The fundamentals of HEM were presented in Chapter 3. However, it has been in Chapter 4 that the application of HEM to EDP was detailed. For this purpose, a simple example was presented highlighting the use of the technique used in the dissertation. A simple generic example shows how the formulation of the HEM problem occurs and how it was solved step by step. In this sense, a restarted HEM was explained and illustrated its difference comparing with the HEM itself. Besides the nonlinear equations that describe the EDP, it was demonstrated how the equations are embedded and how the Taylor's power series were calculated. Based on these coefficients, a Padé approximant was calculated. The polynomial of the Taylor's series was limited to a maximum degree, in general no more than degree 9. In case of inadequate convergence until this order, the process is restarted. The restarted process

consists in performing another series computations, however, using the germ solution as the latter Padé approximant result computed for a unitary scaling factor.

The HEM-EDP approach was studied through experiments in 3-, 9- and 14-bus test systems. Each studied system was submitted under three different scenarios. Namely, a conservative, that presented average loading and relaxed limits; a moderate, with 20% higher loading in relation to the moderate scenario, and relaxed limits; and a radical scenario, also with 20% higher loading in relation to the moderate scenario, however with more strict limits.

The experiment results from the alternative approach were then compared with the results obtained from the traditional iterative technique, Newton-Raphson. For all studied cases and scenarios, the HEM-EDP approach presented a better accuracy than the NR method. In fact, at every partial solution, the HEM-EDP also presented a better overall accuracy. Another important point to be featured is the robustness of the method. In view of its restarted characteristics, it enables smaller order Taylor series, and smaller coefficients values. Then providing faster and less computational burden.

6.2 Future Works

Future works in this topic can be exploited. We suggest for instance, incorporation of new constrains by considering other operational limits, such as power flow at interconnection circuits, voltage phases etc. Another constrain would be the introduction of maximum limit for the power injected into a specified bus. Also, other aspects might be incorporated into the objective function, expanding the optimization options in this function. One example would be to include transmission losses, which in this dissertation were treated only as part of the equality constraints in the power balance equation.

As there are many possibility to holomorphically embed the nonlinear equations, this theme still deserves more investigations, as well as a new alternative methods to compute the Taylor's power series associated to the problem of interest.

Bibliography

- [1] Loau Tawfak Al Bahrani, Jagdish C. Patra and Ryszard Kowalczyk, "Multi-Gradient PSO Algorithm for Economic Dispatch of Thermal Generating Units in Smart Grid," 2016 IEEE Innovative Smart Grid Technologies - Asia (ISGT-Asia), Melbourne, VIC, 2016, pp. 258-263.
- [2] F. Benhamida, I. Ziane, S. Souag, A. Graa and B. Dehiba, "Solving Dynamic Economic Load Dispatch With Ramp Rate Limit Using Quadratic Programming," 2013 North American Power Symposium (NAPS), Manhattan, KS, 2013, pp. 1-5.
- [3] Y. Adhinarayanan and M. Sydulu, "Fast and Effective Algorithm for Economic Dispatch of Cubic Fuel Cost Based Thermal Units," First International Conference on Industrial and Information Systems, Peradeniya, 2006, pp. 156-160.
- [4] Ahmed Yousuf Saber, "Economic Dispatch Using Particle Swarm Optimization With Bacterial Foraging Effect," in Electrical Power And Energy Systems, International Journal of Electrical Power & Energy Systems, vol. 34, pp. 38-46, 2012.
- [5] James A. Momoh, Roger F. Austin, Rambabu Adapa and E. C. Ogbuobiri, "Application of Interior Point Method to Economic Dispatch," [Proceedings] 1992 IEEE International Conference on Systems, Man, and Cybernetics, Chicago, IL, USA, 1992, pp. 1096-1101 vol.2.
- [6] C. Wu and C. Cao and J. Xie and D. Yue and S. Xu and J. Wang, "Economic dispatch of virtual power plant based on distributed primal-dual sub-gradient method," 2017 36th Chinese Control Conference (CCC), pp.10517-10521, July 2017.
- [7] Anup Shukla, James A. Momoh and S. N. Singh, "Unit Commitment using Gravitational Search Algorithm with Holomorphic Embedded Approach," 2017 19th International Conference on Intelligent System Application to Power Systems (ISAP), San Antonio, TX, 2017, pp. 1-6.

-
- [8] T. Yalcinoz and H. Altun, "Power Economic Dispatch Using a Hybrid Genetic Algorithm," in *IEEE Power Engineering Review*, vol. 21, no. 3, pp. 59-60, March 2001.
- [9] A. Trias, "The Holomorphic Embedding Load-Flow Method," *Power and Energy Society General Meeting*, pp. 1-8, July 2012.
- [10] Shuruti Rao and Daniel Tylavsky, "Nonlinear Network Reduction for Distribution Networks using the Holomorphic Embedding Method," *2016 North American Power Symposium (NAPS)*, Denver, CO, 2016, pp. 1-6.
- [11] F. D. Freitas, A.C. Santos and L. F. J. Fernandes, "Restarted Holomorphic Embedding Load-Flow Model Based on Low-Order Padé Approximant and Estimated Bus Power Injection," *International Journal of Electrical Power and Energy Systems*, v. 112, pp. 326-338, Nov. 2019.
- [12] S. Rao, Y. Feng, D. J. Tylavsky and M. K. Subramanian, "The Holomorphic Embedding Method Applied to the Power-Flow Problem," in *IEEE Transactions on Power Systems*, vol. 31, no. 5, pp. 3816-3828, Sept. 2016.
- [13] Anup Shukla, Saurabh Keshewani and S. N. Singh, "Efficient Holomorphic Based Approach for Unit Commitment Problem," *2016 National Power Systems Conference (NPSC)*, Bhubaneswar, 2016, pp. 1-6.
- [14] Rui Yao, Kai Sun, Di Shi and Xiaohu Zhang, "Voltage Stability Analysis of Power Systems With Induction Motors Based on Holomorphic Embedding," in *IEEE Transactions on Power Systems*, vol. 34, no. 2, pp. 1278-1288, March 2019.
- [15] Senthil Krishnamurthy and Raynitchka Tzoneva, "Investigation on the Impact of the Penalty Factors over Solution of the Dispatch Optimization Problem," *2013 IEEE International Conference on Industrial Technology (ICIT)*, Cape Town, 2013, pp. 851-860.
- [16] Salih Fadil and Burak Urazel, "Application of Modified Subgradient Algorithm Based in Feasible Values to Security Constrained Economic Dispatch Problem with Prohibited Operation Zones," *2013 8th International Conference on Electrical and Electronics Engineering (ELECO)*, Bursa, 2013, pp. 549-553.
- [17] X. S. Han, H. B. Gooi and Daniel S. Kirschen, "Dynamic Economic Dispatch: Feasible Optimal Solutions," *IEEE Transactions on Power Systems* 2001, vol. 16, no. 1.

-
- [18] Z. Liang and J. D. Glover "A zoom feature for adynamic programming solution to economic dispatch including transmission losses," IEEE Transactions on Power Systems, vol. 7, no.2, p. 544-550, May 1992.
- [19] S. P. Agrawal, K. B. Porate and G. H. Raisonni "Economic Dispatch of Thermal Units with the Impact of Wind Power plant," 3 International Conference on Emerging Trends in Engineering and Technology, Goa, 2010, pp. 48-53.
- [20] B. F. Wollenberg, A. J. Wood and G. B. Sheble, "Power Generation Operation and Control," Chapter 4, Third Edition, 2013.
- [21] Tohei Shiokawa and Teruhisa Kumano, "A new fuel cost model of thermal unit considering output ramp rate and its application to Economic Load Dispatch," 2009 IEEE Electrical Power and Energy Conference (EPEC), Montreal, QC, 2009, pp. 1-6.
- [22] T. Kumano, "A Function Optimization Based Dynamic Economic Load Dispatch Considering Ramping Rate of Thermal Units Output," 2011 IEEE/PES Power Systems Conference and Exposition, Phoenix, AZ, 2011, pp. 1-8.
- [23] , J. J. Grainger and W. D. Stevenson, "Power System Analysis", McGraw-Hill, 1994.
- [24] B. J. Parker, A. Watanabe and M. T. Schiling, "Precisão do Modelo Linearizado de Fluxo de Potência para Simulação do Sistema Elétrico Brasileiro," NT DEST 18/80.
- [25] Y. Li, "Effect of Various Holomorphic Embeddings on Convergence Rate and Condition Number as Applied to the Power Flow Problem." Master Thesis, Arizona State University, Nov. 2015.
- [26] E. D. Castronuovo, "Aplicação de métodos de pontos interiores no fluxo de potência ótimo não-linear com utilização de processamento de alto desempenho," 2001, UFSC, Tese Doutorado.
- [27] Khalid Mohamed-Nor, Abdul Halim and Abdul Rashid, "Efficient economic dispatch algorithm for thermal unit commitment,"in IEE Proceedings C - Generation, Transmission and Distribution, vol. 138, no. 3, pp. 213-217, May 1991.
- [28] A. Trias, "Fundamentals of the Holomorphic Embedding Load-Flow Method," ArXiv e-prints, no. 1509.02421, Sep. 2015.

-
- [29] M. K. Subramanian, Y. Feng and D. Tylavsky, "PV Bus Modeling in a holomorphically Embedded Power-Flow Formulation," North American Power Symposium (NAPS), Manhattan, KS, 2013.
- [30] A. Trias and J. L. Marín, "The Holomorphic Embedding Loadflow Method for DC Power Systems and Nonlinear DC Circuits," IEEE Trans. Circuits Syst. I, Reg. Papers, vol. 63, no. 2, pp. 322-333, Feb. 2016.
- [31] R. D. Zimmerman, C. E. Murillo-Sánchez, and R. J. Thomas, "MATPOWER: Steady-State Operations, Planning and Analysis Tools for Power Systems Research and Education," IEEE Trans. Power Syst., vol.26, no. 1, pp. 12-19, Feb. 2011.
- [32] P. Murty, "Power Systems Analysis." Hyderabad, India: BSP, 2007.
- [33] J. Arrillaga and C. P. Arnold, "Computer Analysis of Power Systems." Christchurch, New Zealand: John Wiley & Sons, 1990.
- [34] Expósito, A.G.; Gomez, E.A.; Conejo, A.J.; Canizares, C. "Electric Energy Systems: Analysis and Operation." CRC Press: Boca Raton, FL, USA, 2009.
- [35] G. W. Stagg A. El-Abiad "Computer Methods in Power System Analysis." in New York: McGraw-Hill 1968.
- [36] L. L. Grigsby "Power Systems." in New York: CRC Press 2006.
- [37] H. Saadat, "Power System Analysis." McGraw-Hill, 2010.
- [38] J. D. Glover, M. S. Sarma and T. J. Overbye, "Power System Analysis and Design 5th Edition," Cengage Learning, Stamford, 2011.
- [39] A. Göran "Power System Analysis." EEH - Power Systems Laboratory, ETH Zürich, Sep. 2012.
- [40] S.P. Suetin, "Padé Approximants and the Effective Analytic Continuation of a Power Series," Russian Math. Surveys, 57:1 (2002), 43-141.
- [41] I.J.Nagrath D.P.Kothari "Modern Power System Analysis." Tata Mcgraw-Hill Newdelhi India 2003.
- [42] Ahlfors L.V., "Complex Analysis: an Introduction to the Theory of Analytic Functions of One Complex Variable," McGraw-Hill, 1979.

-
- [43] Golub, G.H. and Von Loan, C.F., "Matrix computations," The Johns Hopkins University Press, Third Edition, London, UK, 1996.
- [44] Salih Fadil, Ahmet Yazici and Burak Urazel, "Solution to Security Constrained Lossy Economic Power Dispatch Problem for a Power System Are Including Energy Supply Thermal Units Using Modified Subgradient Algorithm Based on Feasible Values," 2011 7th International Conference on Electrical and Electronics Engineering (ELECO), Bursa, 2011, pp. 33-37.
- [45] Jarurote Tippayachai, Weerakorn Ongsakul and Issarachai Ngamroo, "Parallel Micro Genetic Algorithm for Constrained Economic Dispatch," in IEEE Transactions on Power Systems, vol. 17, no. 3, pp. 790-797, Aug. 2002.
- [46] Maheswarapu Sydulu, "A very fast and effective non-iterative " λ -Logic based" algorithm for economic dispatch of thermal units," Proceedings of IEEE. IEEE Region 10 Conference. TENCON 99. 'Multimedia Technology for Asia-Pacific Information Infrastructure' (Cat. No.99CH37030), Cheju Island, South Korea, 1999, pp. 1434-1437 vol.2.
- [47] Xiu Xu, Chengxi Liu and Kai Sun, "A Holomorphic Embedding Method to Solve Unstable Equilibrium Points of Power Systems," 2018 IEEE Conference on Decision and Control (CDC), Miami Beach, FL, 2018, pp. 1580-1585.
- [48] Rin Wang, Chengxi Liu and Kai Sun, "Multi-Stage Holomorphic Embedding Method for Calculating the Power Voltage Curve," in IEEE Transactions on Power Systems, vol. 33, no. 1, pp. 1127-1129, Jan. 2018.
- [49] Masahico Tanimoto, Yoshio Izui, Koichi Hirose and Shizuka Nakamura, "Advanced Economic Dispatching Control Algorithm Using Dynamic Unit Model and Interior Point Method," 1997 Fourth International Conference on Advances in Power System Control, Operation and Management, APSCOM-97. (Conf. Publ. No. 450), Hong Kong, 1997, pp. 796-801 vol.2.
- [50] Xihui Yan and Victor H. Quintana, "An Efficient Predictor-Corrector Interior Point Algorithm for Security Constrained Economic Dispatch ,"in IEEE Transactions on Power Systems, vol. 12, no. 2, pp. 803-810, May 1997.
- [51] G. Irisarri, L. M. Kimball, K. A. Clements, A. Bagchi and P. W. Davis, "Economic Dispatch With Network and Ramping Constraints via Interior Points Method,"in IEEE Transactions on Power Systems, vol. 13, no. 1, pp. 236-242, Feb. 1998.

-
- [52] Kyoung-Shin Kim, Leen-Hark Jung, Seung-Chul Lee and Un-Chul Moon, "Security Constrained Economic Dispatch Using Interior Point Method,"2006 International Conference on Power System Technology, Chongqing, 2006, pp. 1-6.
- [53] F. Z. Gherbi and F. Lakdja, "Environmentally Constrained Economic Dispatch via Quadratic Programming,"2011 International Conference on Communications, Computing and Control Applications (CCCA), Hammamet, 2011, pp. 1-5.
- [54] Nagarjuna Duvvuru and K. S. Swarup, "A Hybrid Interior Point Assisted Differential Evolution Algorithm for Economic Dispatch,"in IEEE Transactions on Power Systems, vol. 26, no. 2, pp. 541-549, May 2011.
- [55] Dhivya S. and Vigneswaran T., "Primal Dual Interior Point Algorithm for Constrained Economic Load Dispatch and Optimal Power Flow," 2013 International Conference on Power, Energy and Control (ICPEC), Sri Rangalatchum Dindigul, 2013, pp. 360-365.
- [56] Z. L. Wu, Q. H. Wu, X. X. Zhou and M. S. Li, "Hybrid Quadratic Programming and Compact Formulation Method for Economic Dispatch with Prohibited Operating Zones and Network Losses,"2015 IEEE Innovative Smart Grid Technologies - Asia (ISGT ASIA), Bangkok, 2015, pp. 1-6.
- [57] M. S. P. Subathra, S. Easter Selvan, T. Aruldoss Albert Victoire, A. Hepzibah Christinal and Umberto Amato, "A Hybrid with Cross-Entropy Method and Sequential Quadratic Programming to Solve Economic Load Dispatch Problem ,"in IEEE Systems Journal, vol. 9, no. 3, pp. 1031-1044, Sept. 2015.
- [58] Ismail Ziane, Farid Benhamida, Yacine Salhi and Amel Graa, "A Fast Solver for Dynamic Economic Load Dispatch with Minimum Emission Using Quadratic Programming,"2015 4th International Conference on Systems and Control (ICSC), Sousse, 2015, pp. 290-294.
- [59] Rony Seto Wibowo, Kemas Robby Firmansyah, Ni Keut Aryani and Adi Seoprijanto, "Dynamic Economic Dispatch of Hybrid Microgrid with Energy Storage Using Quadratic Programming,"2016 IEEE Region 10 Conference (TENCON), Singapore, 2016, pp. 667-670.
- [60] Nnamdi Nwulu, "Emission Constrained Bid based Dynamic Economic Dispatch using Quadratic Programming," 2017 International Conference on Energy, Communication, Data Analytics and Soft Computing (ICECDS), Chennai, 2017, pp. 213-216.

-
- [61] M. R. B. D. Santos, A. R. Balbo, E. Gonçalves, E. M. Soler, R. B. N. M. Pinheiro, L. Napomuceno and E. C. Baptista, "A Proposed Methodology Involving Progressive Bounded Constraints and Interior-Exterior Methods in Smoothed Economic/Environmental Dispatch Problems," in IEEE Latin America Transactions, vol. 15, no. 8, pp. 1422-1431, 2017.
- [62] J. Lin and F. H. Magnago, "Electricity Markets: Theories and Applications," Chapter 5, First Edition, 2017.
- [63] R. N. Dhar and P. K. Mukherjee, "Reduced-Gradient Method for Economic Dispatch," in Proceedings of the Institute of Electrical Engineers, Volume 120, pg. 608-610, May 1973.